

Boosting Multimodal Reasoning with Automated Structured Thinking

Jinyang Wu^{1*} Mingkuan Feng^{1*} Shuai Zhang^{1†} Fangrui Lv¹
 Ruihan Jin¹ Feihu Che² Zhengqi Wen² Jianhua Tao^{12†}

¹ Department of Automation, Tsinghua University

² Beijing National Research Center for Information Science and Technology
 wu-jy23@mails.tsinghua.edu.cn, zhang_shuai@mail.tsinghua.edu.cn

Abstract

Multimodal large language models excel across diverse domains but struggle with complex visual reasoning tasks. Current approaches aim to incorporate structured thinking via two strategies: explicit search methods and post-training techniques. However, both approaches face significant limitations: Search-based methods suffer from computational inefficiency due to extensive solution space exploration, while post-training methods require substantial data, computational resources, and often encounter training instability. To address these limitations, we propose AStar, an **Automated Structured thinking** paradigm for multimodal reasoning. Our method introduces “*thought cards*”, a lightweight library of high-level reasoning patterns abstracted from 500 prior samples using Monte Carlo Tree Search. For each test problem, AStar adaptively retrieves the optimal thought cards and seamlessly integrates these external explicit guidelines with the model’s internal implicit reasoning capabilities. Extensive experiments demonstrate AStar’s effectiveness and efficiency: using only 500 prior samples and a 7B backbone, our training-free framework achieves 53.9% accuracy on MathVerse (surpassing GPT-4o’s 50.2%) and 32.7% on MathVision (versus GPT-4o’s 30.4%). Further analysis reveals that AStar generalizes beyond multimodal reasoning to visual perception and understanding domains, and serves as a plug-and-play test-time inference method compatible with mainstream post-training techniques like GRPO.

1 Introduction

Multimodal Large Language Models (MLLMs) have demonstrated impressive capabilities across diverse tasks and domains [1–3], yet they struggle with complex visual reasoning tasks that require processing multimodal information with sophisticated problem-solving strategies [4, 5]. Recent advances in System 2 slow-thinking reasoning models like OpenAI-o1 [6], DeepSeek-R1 [7], and Kimi-K1.5 [8] have inspired growing interest in incorporating structured long Chain-of-Thought (CoT) [9] thinking into MLLMs [10–12]. These approaches address limitations of conventional MLLMs that often rely on simple “direct prediction” modes due to the scarcity of high-quality long-chain reasoning data [10, 13]. Current methods can be divided into two primary categories: (i) *explicit search methods* [14, 15]: leverage algorithms like beam search or Monte Carlo Tree Search (MCTS) with specialized reward models to guide extensive solution path exploration; (ii) *post-training methods* [1, 16]: develop structured long CoT reasoning capabilities through common techniques such as large-scale Supervised Fine-Tuning (SFT) [4, 13] or Reinforcement Learning with Verifiable Rewards (RLVR) like Group Relative Policy Optimization (GRPO) [17, 18].

* Equal contributions.

However, both kinds of methods face some limitations. (i) Search-based methods [14] suffer from computational inefficiency due to extensive exploration across solution spaces; (ii) SFT-based post-training methods [13, 15, 19] typically require substantial training data ($\geq 100K$) and computational resources to implicitly extract reasoning patterns, leading to inefficient data utilization. Their reliance on proprietary models like GPT-4o for data synthesis also creates accessibility barriers for researchers outside major enterprises; (iii) RLVR-based post-training methods [20, 21] encounter challenges with exploration depth and training stability. As shown in [22, 23], these methods primarily function by biasing the model’s output distribution toward reward-maximizing paths without introducing external knowledge. This inherently limits their exploration capacity, resulting in a narrower reasoning capability boundary compared to base models.

To address these limitations, we propose AStar, an **Automated Structured thinking** paradigm for multimodal reasoning. AStar introduces a novel and versatile reasoning framework that seamlessly combines MLLMs’ internal implicit reasoning capabilities with external explicit reasoning guidelines. Specifically, we design “*thought cards*”, a general and lightweight library storing abstract high-level thoughts (*atomic reasoning action-guided reasoning guidelines*), which are abstracted from only 500 prior samples using MCTS and can be generalized across tasks. For each test problem, we adaptively retrieve five optimal thought cards aligned with the problem’s characteristics (complexity and semantics). With these abstract guidelines, we perform visual reasoning and obtain the final solution with unified self-consistency checks and outcome reward scoring.

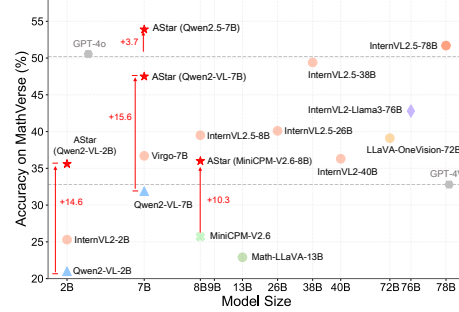


Figure 1: Evaluation results on MathVerse. AStar makes 7B models competent problem-solvers, surpassing GPT-4o. Our approach demonstrates consistent effectiveness across multiple model architectures and scales.

Our method offers four key advantages: (i) **Performance Enhancement**: By leveraging high-level thought cards, we adaptively obtain reasoning guidelines based on problem attributes, integrating external guidance with the model’s internal capabilities, thereby enhancing performance (Figure 1); (ii) **Efficiency Improvement**: Our training-free framework achieves comparable performance to powerful baselines with only 500 prior samples, enhancing both data and computational efficiency; (iii) **Scalability and Flexibility**: Thought cards can be rapidly constructed for new tasks using minimal task-relevant data; and (iv) **Generalization and Plug-and-Play Capability**: Beyond multimodal reasoning, our framework benefits general visual perception and understanding tasks. It can also function as a plug-and-play test-time inference method compatible with popular post-training techniques like SFT and GRPO. We summarize our core contributions as follows:

- We introduce an adaptive training-free reasoning framework that combines MLLMs’ internal implicit capabilities with external explicit guidelines, achieving both effectiveness and efficiency.
- We propose “thought cards” for storing informative high-level thoughts abstracted from minimal prior samples, which can be adaptively instantiated for specific test problems.
- We conduct extensive experiments across multimodal reasoning, visual perception and understanding tasks. Our method AStar achieves 53.9% accuracy on MathVerse (versus GPT-4o’s 50.2%) and 32.7% on MathVision (versus GPT-4o’s 30.4%) with only 500 prior samples and a 7B inference backbone. Results on BLINK and MMMU also demonstrate generalizability to broader visual perception and understanding tasks. Moreover, this framework can be effectively integrated with popular post-training techniques like GRPO for further performance enhancements.

2 Methodology

Overview of AStar This section introduces our proposed method AStar in detail. As shown in Figure 2 and Algorithm 1, our approach consists of three steps:

- *Visual Reasoning Action Definition*: Establish six human-like reasoning actions as building blocks for chain-structured thought cards.

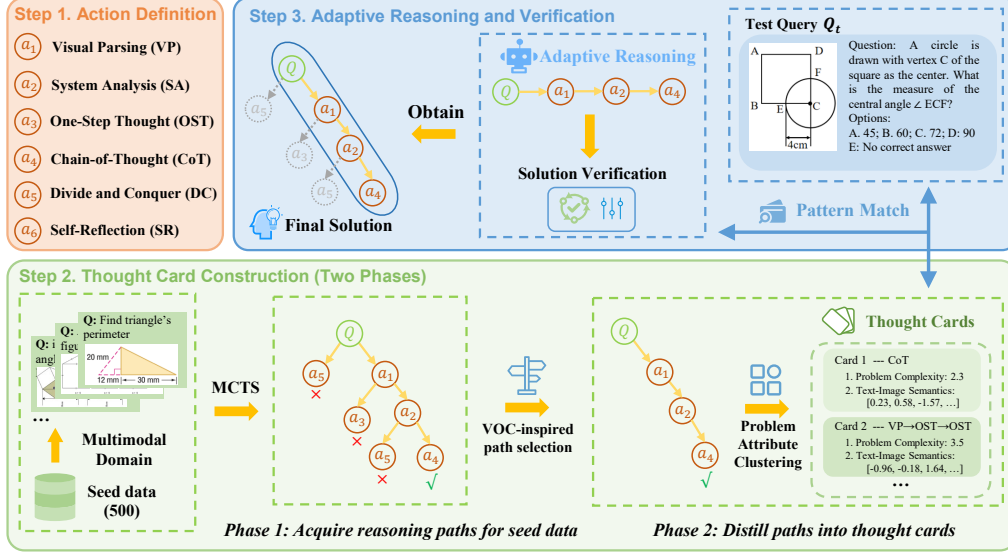


Figure 2: Flowchart of our method AStar. This framework consists of three parts: (1) Visual Reasoning Action Definition; (2) Thought Card Construction; (3) Adaptive Reasoning and Verification.

- *Thought Card Construction:* Leverage MCTS to systematically construct thought cards, which serve as reference insights and effectively guide subsequent problem-solving during inference.
- *Adaptive Reasoning and Verification:* Dynamically select and execute optimal reasoning patterns based on problem complexity, followed by robust solution verification.

2.1 Visual Reasoning Action Definition

Understanding human complex reasoning is crucial for modeling cognitive processes [24]. Existing studies distinguish between two cognitive systems: System 1 and System 2 [25, 26]. While “System 1” represents fast, intuitive, yet error-prone thinking, “System 2” involves slow, deliberative thinking with superior performance. With the emergence of advanced models like OpenAI o1 [6] and Kimi-K1.5 [8], developing efficient “System 2” approaches to emulate human cognitive processes has gained significant research attention [15, 27, 28]. Inspired by this, we introduce six vision-language reasoning actions to bridge the gap between model reasoning and human cognition: *Visual Parsing* (VP, a_1), *System Analysis* (SA, a_2), *One-Step Thought* (OST, a_3), *Chain-of-Thought* (CoT, a_4), *Divide and Conquer* (DC, a_5), *Self-Reflection* (SR, a_6). Details are provided in Appendix C.1.

2.2 Thought Card Construction

Based on the above action definitions, we introduce “*thought cards*” as reasoning templates to guide inference in Section 2.3. Using only 500 prior samples, we first derive their reasoning paths (Phase 1) and then distill them into high-level thought cards (Phase 2). These cards provide structured guidance for efficient problem-adaptive reasoning during inference.

Phase 1: Acquire reasoning paths for seed data As shown in Figure 2, we employ MCTS to iteratively optimize the solution search process, generating high-quality reasoning paths for the seed dataset. This design leverages MCTS’s systematic exploration and MLLMs’ inherent reasoning capabilities [29, 1]. We formulate each multimodal reasoning problem x (consisting of input question and images) as a tree search problem, where x represents the root node and subsequent nodes denote reasoning steps (actions and corresponding outcomes) generated by a policy MLLM π_θ . We define the state S_{t-1} as the trajectory x, s_1, \dots, s_{t-1} , where $S_0 = x$. The next step is sampled as $s_t \sim \pi_\theta(S_{t-1})$. To guide tree expansion, we define $Q(s)$ as the reward value for node s . Initially, all unexplored nodes are assigned $Q(s_i) = 0$. They are updated using a weighted average between the parent’s current value and its child node’s value:

$$Q(p) \leftarrow (1 - \alpha)Q(p) + \alpha Q(s) \quad (1)$$

Algorithm 1 Multimodal Reasoning with AStar

Input: a policy model π_θ ; a multimodal test query x_t ; a set of seed data D_s

- 1: Initialize action space $A = \{a_1, a_2, a_3, a_4, a_5, a_6\}$ \triangleright 2.1. Action Definition
- 2: Initialize repository $D \leftarrow []$; Cards $\mathbb{C} \leftarrow \{\}$
- 3: **for** $(x, y) \in D_s$ **do** \triangleright 2.2. Thought Card Construction
- 4: Acquire reasoning paths $\{x, P\} \leftarrow \text{MCTS}(\pi_\theta; x)$
- 5: **if** found at least one valid reasoning path **then**
- 6: Find p_{best} from P (Equation (3))
- 7: Add $\{x, p_{\text{best}}\}$ into D
- 8: Update \mathbb{C} from D
- 9: **end if**
- 10: **end for**
- 11: $\mathbb{C}_{x_t} \leftarrow \text{Card_Match}(\mathbb{C}; x_t)$ \triangleright 2.3. Adaptive Reasoning and Verification
- 12: $y_t \leftarrow \text{Reason_And_Verify}(\pi_\theta; x_t; \mathbb{C}_{x_t})$

Output: the optimal reasoning trajectory y_t

where α is a discount factor for future rewards. For terminal nodes, we adopt the likelihood of self-consistency majority voting as reward value, enabling supervision-free generalization. Specifically, this phase comprises four MCTS operations:

(1) *Selection*. This operation identifies promising nodes for expansion. Starting from the root node, we iteratively select child nodes using the Upper Confidence Bounds applied to Trees (UCT) [30] until reaching a leaf node:

$$UCT(s) = Q(s) + w \sqrt{\frac{\ln N(p)}{N(s)}} \quad (2)$$

where $Q(s)$ is the reward value for node s , $N(s)$ is the visit count, p is the parent node, and w is the exploration weight. The node with the highest UCT value is selected for subsequent phases, balancing exploration and exploitation.

(2) *Expansion*. The selected node s is expanded by sampling n actions from π_θ and generating corresponding reasoning outcomes. These n child nodes are added to the tree and stored in an external memory structure.

(3) *Simulation*. Starting from the selected node, we iteratively sample and expand nodes until reaching a terminal state (maximum depth or final answer node).

(4) *Backpropagation*. Upon simulation completion, node information is updated along the simulation path s_0, \dots, s_d . Visit counts are incremented ($N(s) \leftarrow N(s) + 1$), and node value $Q(s)$ is propagated backward to its parent node p using Equation 1. These updated values are used to guide subsequent UCT-based node selection.

Phase 2: Distill paths into thought cards After executing MCTS, we obtain a tree structure for each seed dataset question, yielding multiple valid reasoning paths that constitute the path set P . Inspired by the concept of Value of Computation (VOC) [31], which optimizes the trade-off between computational benefits and costs, we propose a VOC-inspired selection metric to identify the optimal reasoning trajectory from candidate solutions:

$$\text{Score}(x, p_x) = k \cdot R(p_x|x) - (1 - k) \cdot C(p_x) \quad (3)$$

where x is the task input, $p_x \in P$ denotes a candidate reasoning path, and k balances benefits against computational costs. Here, $R(p_x|x)$ denotes the path’s final reward (defined as the leaf node’s Q-value), while $C(p_x)$ is the reasoning cost (defined as the number of actions in the sequence).

Then, for each question in the seed dataset, we select the path p_{best} with the highest $\text{Score}(x, p_x)$ to build a *Question-path repository* D with one-to-one mappings. Inspired by metareasoning principles [31, 32], which advocate for adaptive reasoning strategies, we distill these question-path pairs into abstract thought cards \mathbb{C} as high-level guidelines. Each card is distilled based on two attributes: problem condition complexity (PCC) [33] and text-image semantics (TIS) [14, 34]. PCC represents prior known conditions derived from input image-text pairs (i, t) , obtained using a lightweight 2B

MLLM. TIS refers to joint semantic representations based on the CLIP model encodings of (i, t) :

$$E_x(i, t) = \frac{E_I(i) + E_T(t)}{2} \quad (4)$$

Finally, each thought card contains a high-level thought template (e.g., $a_1 \rightarrow a_2 \rightarrow a_4$), along with the average problem complexity and text-image semantics of multiple questions sharing this template.

2.3 Adaptive Reasoning and Verification

During inference, given a multimodal test query x_t , we compute its PCC and TIS, and perform nearest neighbor matching [35] against pre-constructed thought cards \mathbb{C} to identify the five most relevant cards that best align with its complexity level and semantics. The selection process involves ranking cards based on similarity for each attribute independently:

$$R_{\text{TIS}}(c) = \text{Rank} \left(E_{x_t}(i_t, t_t)^\top E_x(i_c, t_c) \right), \forall c \in \mathbb{C} \quad (5)$$

$$R_{\text{PCC}}(c) = \text{Rank} \left(\frac{1}{|PCC_{x_t} - PCC_c|} \right), \forall c \in \mathbb{C} \quad (6)$$

where $\text{Rank}(\cdot)$ assigns rankings in descending order, with higher values receiving better rankings (e.g., the highest value is ranked 1, the lowest value is ranked $|\mathbb{C}|$). We then combine these rankings to compute a total ranking score:

$$R(x_t, c) = R_{\text{TIS}}(c) + R_{\text{PCC}}(c) \quad (7)$$

Finally, we select the five thought cards with better combined rankings:

$$NN_5(x_t, \mathbb{C}) = \arg \min_{\mathbb{C}_{x_t} \subseteq \mathbb{C}, |\mathbb{C}_{x_t}|=5} \sum_{c \in \mathbb{C}_{x_t}} R(x_t, c) \quad (8)$$

where $\mathbb{C}_{x_t} \subseteq \mathbb{C}$ contains the five thought cards with the best combined rankings. We instantiate these templates for the test query to obtain five candidate solutions. To identify the best reasoning trajectory, we employ both self-consistency checks and text-domain outcome reward models due to the scarcity of visual-domain verification models. Details are described in Appendix B.4.

In summary, our approach adaptively selects high-level reasoning guidelines based on problem attributes, elegantly integrating the model’s internal implicit reasoning capabilities with external explicit guidance. This dynamic selection mechanism enables more flexible and efficient reasoning across diverse problem types while maintaining robust performance.

3 Experiments

The section presents 3.1 Experimental Setup and assesses AStar from four aspects: 3.2 Performance, 3.3 Efficiency, 3.4 Out-of-Distribution Generalization, and 3.5 Ablation Study and Analysis.

3.1 Experimental Setup

Datasets We perform extensive experiments across three tasks and eight datasets: (1) mathematical reasoning: MathVista [36], MathVerse [37], and MathVision [5]; (2) commonsense and scientific reasoning: GAOKAO-MM [38]; (3) general visual perception and understanding: ChartQA [39], MMStar [40], MMMU [41] and BLINK [42]. For all benchmarks, we adopt the official evaluation metrics. Further details can be found in Appendix D.1.

Models To demonstrate AStar’s versatility, we evaluate its effectiveness on both LLM and MLLM, including Qwen2.5-7B [43], and Qwen2-VL-2/7B [44]. This design aims to validate that AStar can seamlessly leverage pre-trained LLM and MLLM as its inference backbone without modifications.

Baselines In this paper, we comprehensively evaluate AStar against four strong and representative baseline categories: (1) open-source general MLLMs, including the powerful Qwen2-VL [45] and InternVL2 series [46]; (2) open-source MLLMs specifically optimized for complex reasoning, such as SFT-based methods URSA [13], Math-LLaVA [47], and RLVR-based methods R1-VL-7B [18], LMM-R1 [20], and MM-Eureka [48]; (3) explicit search-based methods such as Mulberry [15]; and (4) advanced closed-source MLLMs, including GPT-4o [2], and GPT-4V [49].

Table 1: Evaluation of AStar’s reasoning abilities on MathVista and MathVerse *testmini*. The best results are highlighted in **bold**. For MathVerse, we show 7 categories: ALL (overall accuracy), VI (vision intensive), VD (vision dominant), VO (vision only), TD (text dominant), TL (text lite), and TO (text only). For MathVista, we present 5 categories: ALL (overall accuracy), ARI (arithmetic reasoning), LOG (logical reasoning), STA (statistical reasoning), and VQA (visual question answering).

Model	#Params	MathVerse							MathVista				
		ALL	VI	VD	VO	TD	TL	TO	ALL	ARI	LOG	STA	VQA
Random	-	12.4	12.4	12.4	12.4	12.4	12.4	12.4	17.9	13.8	13.4	14.3	26.3
Human	-	64.9	61.4	68.3	66.7	71.2	70.9	41.7	60.3	59.2	40.7	63.9	55.9
<i>Open-Source General MLLMs</i>													
MiniGPT4-7B [50]	7B	12.2	12.5	14.8	8.7	12.3	12.9	13.4	23.1	32.0	10.8	17.9	30.2
LLaVA-1.5-13B [51]	13B	12.7	12.6	12.7	9.0	17.1	12.0	22.6	27.7	28.6	10.8	22.9	30.2
SPHINX-V2-13B [52]	13B	16.1	16.4	15.6	16.2	20.8	14.1	14.0	36.7	33.4	24.3	51.5	43.0
SPHINX-MoE [52]	8×7B	22.8	21.1	19.6	18.3	33.3	21.9	23.1	42.6	43.0	14.4	50.8	43.3
LLaVA-NeXT-34B [53]	34B	34.6	35.2	28.9	22.4	49.0	37.6	30.1	46.5	-	-	-	-
InternLM-XComposer2-VL [54]	7B	25.9	20.1	24.4	19.8	36.9	28.3	42.5	57.6	51.6	13.5	62.8	39.7
Deepseek-VL [55]	7B	19.3	20.2	18.4	11.8	23.0	23.2	23.1	34.9	38.8	18.9	33.2	34.6
InternVL2-8B [46]	8B	35.9	32.2	30.9	27.7	39.0	33.8	36.0	58.3	56.4	10.8	68.8	49.7
Qwen2-VL [45]	7B	33.6	31.3	30.3	28.1	37.4	33.5	35.0	58.9	57.5	24.3	43.1	58.1
<i>Open-Source Math MLLMs (Large-Scale Training)</i>													
G-LLaVA-7B [56]	7B	16.6	17.2	14.6	9.4	20.9	20.7	21.1	25.1	19.4	15.2	15.1	28.7
Math-LLaVA-13B [47]	13B	22.9	24.5	21.7	16.1	27.3	24.9	27.0	46.6	40.7	23.3	42.3	33.5
Math-PUMA-Qwen2-7B [57]	7B	33.6	33.4	31.6	26.0	42.1	35.0	39.8	47.9	46.2	21.6	55.8	30.2
Math-PUMA-DeepSeek-Math [57]	7B	31.8	33.6	31.6	14.7	43.4	35.4	47.5	44.7	41.9	8.1	50.8	31.3
MAVIS-7B [58]	7B	35.2	34.1	29.7	31.8	43.2	37.2	-	-	-	-	-	-
InfMM-Math [59]	7B	34.5	38.1	32.4	15.8	46.7	32.4	-	-	-	-	-	-
MultiMath-7B [60]	7B	27.7	28.1	25.9	15.0	34.8	30.8	35.3	50.0	42.2	23.3	64.9	49.2
URSA-8B [13]	7B	45.7	46.4	43.9	28.6	55.3	48.3	51.8	59.8	53.5	21.6	57.1	40.2
R1-VL-7B [18]	7B	40.0	37.3	33.6	39.8	45.0	40.1	40.7	63.5	54.7	28.5	61.2	60.9
AStar (Qwen2.5-7B, Training-free)	7B	53.9	49.7	64.4	48.6	56.4	48.3	56.1	64.2	63.8	59.5	69.1	60.9
AStar (Qwen2-VL-7B, Training-free)	7B	47.5	41.8	51.6	48.6	49.3	51.0	42.2	61.7	60.6	28.6	68.4	59.6

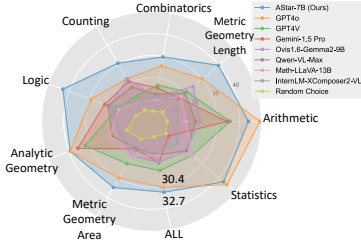


Figure 3: Results on the challenging reasoning benchmark, MathVision. AStar-7B (Qwen2.5-7b) achieves competitive performance to GPT-4o.

Model	Perception		Comprehension	Understanding
	MMStar	BLINK	MMMU	ChartQA
Qwen2-VL-2B	48.0	44.4	41.1	73.5
AStar (Ours, 2B)	52.0	46.7	42.4	78.6
Qwen2-VL-7B	60.7	53.2	54.1	83.0
AStar (Ours, 7B)	61.7	56.0	57.2	83.9

Table 2: Evaluation results on visual perception and understanding benchmarks: (1) Visual Perception: MMStar and BLINK; (2) Context Comprehension: MMMU; (3) Chart Understanding: ChartQA. Our framework generalizes beyond multimodal reasoning to visual perception and understanding domains.

3.2 Performance Comparison with Baselines

Foundational Reasoning Enhancement Analysis Table 1 presents the performance of AStar across two mainstream reasoning benchmarks. We have three key findings:

- AStar consistently outperforms both general and math-specialized MLLMs. With Qwen2.5-7B reasoning backbone, AStar achieves 53.9% accuracy on MathVerse, surpassing large-scale CoT-trained URSA-7B by 8.2%, and the computationally-intensive GRPO-trained R1-VL-7B by 13.9%.
- AStar demonstrates strong performance across diverse reasoning capabilities. It reaches 59.5% on logical reasoning (LOG), outperforming the powerful URSA-7B by 37.9%. Similar gains are observed in statistical reasoning (STA: 69.1%) and visual question answering (VQA: 60.9%).
- AStar’s adaptive reasoning benefits are universal across varying multimodal information distributions. It maintains consistent performance gains from vision-dominant (VD: 64.4%) to text-dominant (TD: 56.4%) and text-only (TO: 56.1%) scenarios, demonstrating robust performance regardless of the modality balance. Notably, its strong performance in the text-only scenario (TO) demonstrates our paradigm’s versatility and ability to generalize beyond multimodal problems to pure text domains.

Table 3: Comparison with two primary methods: search-based methods (Mulberry) and post-training methods (LMM-R1, MM-Eureka, R1-VL, URSA). ‘OS Only’ indicates datasets constructed only with open-source models. As a training-free reasoning framework, AStar achieves superior performance with only 500 prior samples, demonstrating superior efficiency and effectiveness.

Methods	Type	OS Only	Training-Free	Prior Data ↓	MMStar Acc. ↑	MathVerse Acc. ↑	MathVision Acc. ↑
Mulberry-7B [15]	Search	✗	✗	260K	61.3	-	-
URSA-8B [13]	SFT	✗	✗	1100K	55.4	45.7	26.2
LMM-R1-3B [20]	GRPO	✓	✗	55.3K	58.0	41.6	26.4
MM-Eureka-7B [48]	GRPO	✓	✗	15K	59.4	50.3	26.9
R1-VL-7B [18]	GRPO	✓	✗	260K	60.0	40.0	27.1
Ours (Qwen2.5-7B)	-	✓	✓	0.5K	62.3	53.9	32.7
Ours (Qwen2-VL-7B)	-	✓	✓	0.5K	61.7	47.5	26.8

Robust Performance on More Challenging Scenarios As shown in Figure 3, we evaluate AStar against leading models on the challenging MathVision benchmark [5] across multiple reasoning dimensions. AStar achieves 32.7% average accuracy across all dimensions, surpassing GPT-4o (30.4%). Notably, in the logical reasoning area, AStar attains 42.9% accuracy, significantly outperforming GPT-4o (29.4%). AStar’s effectiveness can be attributed to its adaptive problem decomposition framework, which simplifies complex multimodal reasoning tasks into manageable sub-problems, enabling substantial improvements across various reasoning capabilities.

Extending Reasoning Gains to Visual Perception and Understanding To investigate whether our thought-augmented paradigm can generalize to visual perception and understanding tasks, we conduct experiments on four representative benchmarks in Table 2, including visual perception (MMStar [40] and BLINK [42]), contextual comprehension (MMM U [41]), and chart understanding (ChartQA [39]). Results show that our reasoning framework significantly enhances performance across these domains and models of different scales. This reveals that thought-driven structured thinking mechanisms not only benefit complex problem-solving in multimodal reasoning but also strengthen fundamental visual understanding abilities even in less explicitly reasoning-intensive tasks.

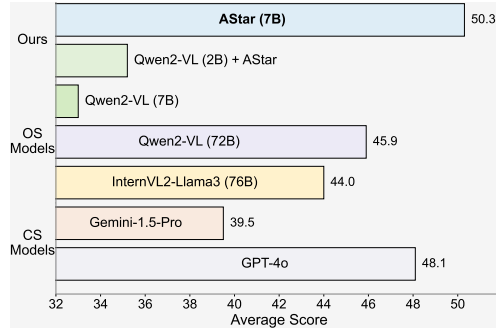


Figure 4: Comparison between AStar and powerful MLLMs across 3 challenging benchmarks: MathVista, MathVerse, and MathVision. ‘OS’ and ‘CS’ denote open-source and closed-source models. AStar with 7B backbone outperforms them.

Achieving Competitive Performance with Smaller Models We further evaluate AStar against leading models across three challenging datasets. As depicted in Figure 4, AStar-7B achieves 50.3% average accuracy across three benchmarks, outperforming GPT-4o (48.1%) and Qwen2-VL-72B (45.9%). Notably, AStar+Qwen2-VL-2B surpasses the larger Qwen2-VL-7B baseline, demonstrating our framework’s ability to elevate smaller models to competitive or superior performance compared to significantly larger architectures. Detailed results are shown in Appendix E.2.

3.3 Data and Computational Efficiency

We further compare AStar with two primary categories of reasoning methods: search-based (Mulberry) and post-training approaches (URSA, LMM-R1, MM-Eureka, R1-VL). Table 3 evaluates these methods across training requirements, open-source compatibility, training data volume, and performance on two tasks: visual understanding (MMStar) and reasoning (MathVerse, MathVision).

Results show AStar achieves superior performance with significantly improved efficiency. Our approach requires only 0.5K prior samples, representing a 520-fold reduction compared to Mulberry (260K) and substantial reductions compared to post-training methods like URSA-8B (110K) and LMM-R1-3B (55.3K). Despite this minimal data requirement, AStar outperforms across all benchmarks: MMStar (62.3% vs. 61.3% for Mulberry), MathVerse (53.9% vs. 45.7% for URSA-8B), and MathVision (32.7% vs. 26.9% for MM-Eureka-7B). Moreover, AStar is fully training-free and built entirely with open-source models, making it accessible for researchers with limited resources. This remarkable efficiency stems from our explicit reasoning pattern extraction strategy, which effectively distills high-level thoughts without extensive training data or computational demands.

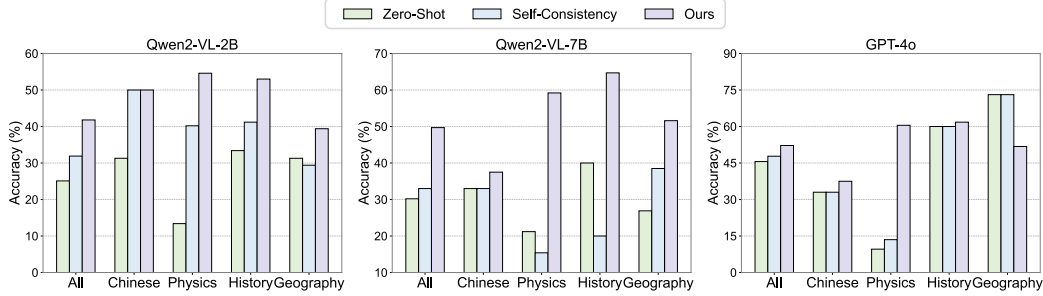


Figure 5: Cross-distribution performance comparison on GAOKAO-MM. We test on Qwen2-VL-2B, Qwen2-VL-7B, and GPT-4o. Results highlight AStar’s superior out-of-distribution performance.

Model Setting	MathVista	MathVerse	Average
AStar	64.2	53.9	59.1
– w/o thought cards (RAC)	59.4	47.9	53.6 ^{-5.5↓}
– w/o card match (RC)	61.7	49.8	55.8 ^{-3.3↓}
– w verification (RS)	62.8	51.7	57.2 ^{-1.9↓}
– w verification (SC)	63.7	52.0	57.9 ^{-1.2↓}

Table 4: Ablation results on AStar-7B (Qwen2.5-7B). ‘RAC’, ‘RC’, ‘RS’, ‘SC’ denotes ‘random action combinations’, ‘random card’, ‘random selection’, and ‘self-consistency’, respectively. We observe that every component is important for optimal performance.

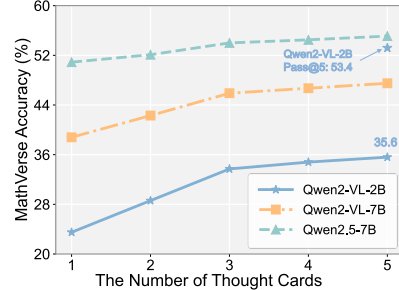


Figure 6: Inference time scaling results.

3.4 Out-of-Distribution Generalization

Recent work has highlighted that distributional shifts severely affect the reliability of MLLMs [29, 61]. While these models excel in in-distribution (ID) tasks, their performance often degrades in out-of-distribution (OOD) scenarios [62]. This challenge is compounded by the inherent difficulty of acquiring sufficient training data and computational resources.

In this section, we evaluate AStar’s performance in OOD scenarios. Since our reasoning guidance during inference is derived from the mathematical domain, we further test on GAOKAO-MM [38], a Chinese human-level multimodal reasoning benchmark that includes historical, geographical, and scientific reasoning tasks. This design naturally constitutes an OOD evaluation setting. As shown in Figure 5, all models demonstrate significant improvements over baseline methods when enhanced with the AStar framework. Notably, for Qwen2-VL-7B, our method improves Geography task accuracy from 26.9% to 51.6% and achieves an average improvement of 19.5% across all subjects. These results validate AStar’s strong generalization across different languages, task distributions, and reasoning domains, establishing it as a robust and versatile approach for both ID and OOD reasoning tasks. Furthermore, we explore additional generalization capabilities in Appendix E.3, including *weak-to-strong generalization*, where we show that our method can even enhance GPT-4o’s performance with weaker models’ guidelines (e.g., Qwen2-VL-7B).

3.5 Ablation Study and Analysis

Ablation Study To investigate the contribution of each component in AStar, we conduct ablation study as shown in Table 4. Here, “w/o” denotes variants with specific components removed. Our analysis reveals three key findings:

First, removing any component leads to performance degradation, validating the necessity of all component designs. Specifically, excluding the card construction module results in the most substantial drops (4.8% on MathVista and 6.0% on MathVerse), highlighting the critical role of thought cards in providing high-level insights for test-time inference.

Second, the precision of card matching also impacts performance, particularly on complex tasks like MathVerse where degradation is more pronounced than on MathVista. While this paper employs PCC-based nearest-neighbor matching, future work could explore more advanced strategies.

Third, while the verification module improves performance, simpler alternatives like random selection (RS) or self-consistency (SC) show only modest degradation (1.9% and 1.2%). This indicates that thought cards enables robust candidate solution generation even with basic selection methods.

Inference Time Scaling We gradually increase the number of selected thought cards during inference to investigate whether our method follows test-time scaling laws. Figure 6 shows that incorporating more reasoning guidelines via thought cards leads to consistent performance improvements.

Plug-and-Play Capability Given that AStar operates as a test-time inference framework, it can be effectively combined with post-training methods. We applied our reasoning paradigm to models that had already undergone post-training procedures (RLVR-trained LMM-R1 [20], i.e., Reinforcement Learning with Verifiable Rewards). As shown in Figure 7, our framework not only seamlessly integrates with these approaches but also consistently enhances their performance. This synergistic effect indicates that AStar could capture unique reasoning patterns complementary to those learned during post-training, further highlighting AStar’s plug-and-play nature. Future work could explore deeper integration with post-training methods to maximize complementary benefits.

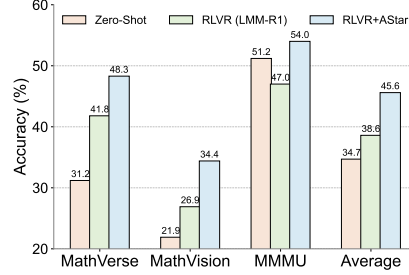


Figure 7: Results on Qwen2.5-VL-3B. AStar integration with RLVR-trained models further enhances performance.

Visualization of Sampling Space To analyze the diversity of solutions generated by our AStar-powered reasoning framework across varying numbers of thought cards, we conduct a visualization study here. We sample 250 problems from MathVision and generate 2 candidate solutions for each problem using AStar (Qwen2-VL-2B), resulting in 500 total samples. Following prior work [14], we employ a three-step analysis process using BGE-M3 [63] for semantic embedding, followed by dimensionality reduction and clustering techniques.

Step 1: Semantic Embedding: We utilize the BGE-M3 encoder f_e to map each answer a_i from our solution set $A = a_1, \dots, a_n$ into a high-dimensional semantic space, producing embedding vectors $\mathbf{e}_i \in \mathbb{R}^d$:

$$\mathbf{e}_i = f_e(a_i), \quad i \in 1, \dots, n \quad (9)$$

where $n = 500$ denotes our total sample size, and d represents the dimension of the embedding space.

Step 2: Dimensionality Reduction: We implement a two-stage dimensionality reduction process, beginning with z-score normalization:

$$\hat{\mathbf{e}}_i = \frac{\mathbf{e}_i - \mu}{\sigma} \quad (10)$$

where μ and σ represent the mean and standard deviation vectors across all embeddings. We then apply PCA to project the standardized embeddings into a two-dimensional space:

$$\mathbf{v}_i = \text{PCA}(\hat{\mathbf{e}}_i) \in \mathbb{R}^2 \quad (11)$$

Step 3: Density-Based Clustering: To identify distinct solution patterns, we apply DBSCAN [64] to the reduced embeddings:

$$C_k = \text{DBSCAN}(\mathbf{v}_i; \epsilon, \text{minPts}) \quad (12)$$

where $\epsilon = 0.7$ defines the neighborhood distance threshold and $\text{minPts} = 4$ specifies the minimum points required for a dense region. C_k denotes the cluster set identified for the number of thought cards k .

Figure 8 and 9 illustrate the visualization results across varying numbers of thought cards ($k = 2$ and $k = 5$) on MathVista and MathVision datasets, respectively. The empirical analysis reveals consistent conclusions across both standard mathematical reasoning tasks (MathVista) and challenging scenarios (MathVision). When fewer thought cards are provided ($k = 2$), the model generates clusters with fewer centroids for the same problem set, indicating a more constrained sampling space with limited potential. Conversely, increasing the number of thought cards to $k = 5$ leads to clusters with more centroids, suggesting a richer sampling space with higher performance potential.

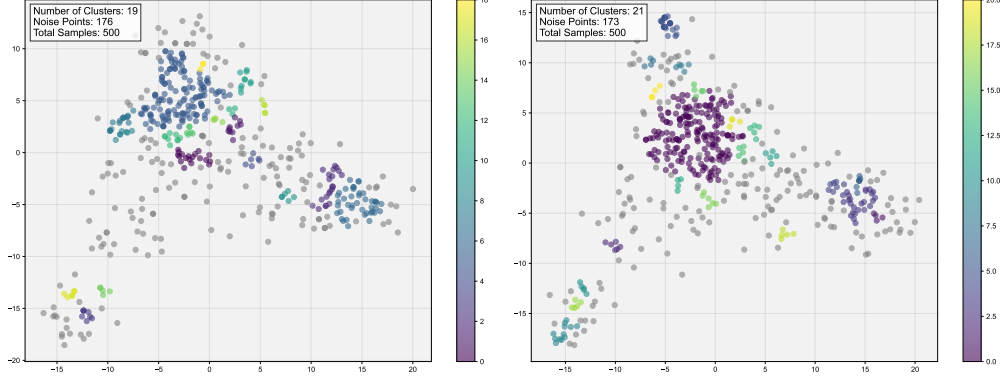


Figure 8: The visualization of candidate reasoning paths across different numbers of thought cards on MathVista. Dots represent individual reasoning steps, while colors indicate distinct solution clusters. The comparison shows results for $k = 2$ (left) and $k = 5$ (right) thought cards, respectively. The increasing density and diversity of clusters from left to right demonstrate the model’s enhanced exploration capability with more thought cards, leading to more comprehensive coverage of the solution space.

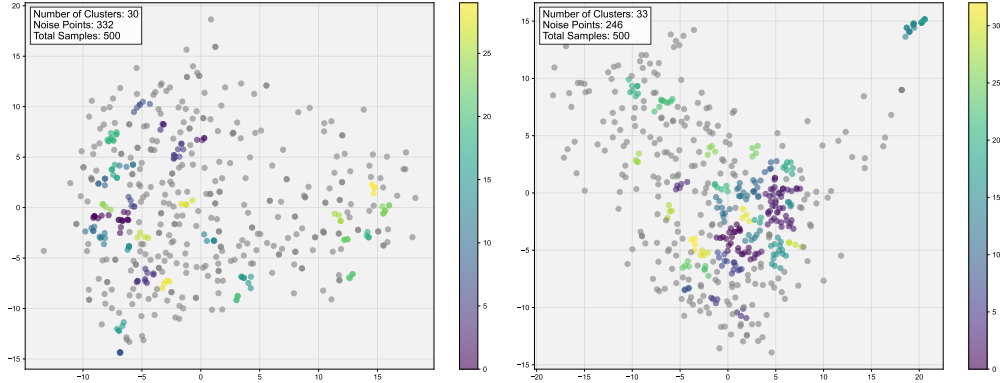


Figure 9: The visualization of candidate reasoning paths across different numbers of thought cards on MathVision. Dots represent individual reasoning steps, while colors indicate distinct solution clusters. The comparison shows results for $k = 2$ (left) and $k = 5$ (right) thought cards, respectively. The increasing density and diversity of clusters from left to right demonstrate the model’s enhanced exploration capability with more thought cards, leading to more comprehensive coverage of the solution space.

Notably, the difference in cluster count between $k = 2$ and $k = 5$ is not particularly large. This observation validates that our framework can effectively adapt to problem complexity by dynamically selecting the most suitable reasoning patterns from high-quality thought cards. Even with fewer thought cards, the framework maintains robust sampling diversity and performance through this adaptive matching mechanism.

Other Analysis Finally, we include some additional results and analysis in the Appendix, including a more comprehensive performance comparison (E.1, E.2), weak-to-strong generalization (E.3), statistical validation (E.4), and case study (F).

4 Related Work

Multimodal Reasoning MLLMs have demonstrated robust capabilities across diverse domains [58, 12, 38]. Despite these achievements, complex multimodal reasoning remains challenging due to its demands on both visual perception and high-level cognition. While recent approaches [10, 27]

implement structured reasoning to enhance CoT capabilities [4], they face inherent limitations: (i) explicit search methods [14, 15] that suffer from computational inefficiency, and (ii) post-training methods [16, 18] that require substantial data and computational resources. These methods either use SFT which shows limited generalization, or employ RLVR like GRPO that lacks the integration of external knowledge [22]. Our work leverages high-level thought cards to seamlessly combine internal model capabilities with external reasoning guidelines. Moreover, many existing approaches employ rigid structures that limit flexibility across different tasks, overlooking the importance of adaptive reasoning in unleashing multimodal reasoning potential [65]. In contrast, our thought cards enable task-specific reasoning paths and adaptive selection, balancing performance with efficiency.

Tree-based Search Tree structures have shown significant potential in language models [66, 67]. Recent research applies these tree-search methods to identify effective reasoning paths for MLLMs. While AR-MCTS [14] enhances multimodal reasoning by integrating MCTS with active retrieval, its extensive iteration and computational demands limit practical applications. Similarly, Mulberry [15] employs tree structures to distill 260K reasoning chains from models like GPT-4o, but requires substantial computational resources and high-capacity teacher models. These methods fail to balance performance with efficiency. To address these limitations, we propose incorporating high-level problem-solving guidelines into MCTS, achieving competitive performance with higher efficiency. While MCTS serves as our reasoning organization structure in this work, our framework is flexible enough to accommodate other advanced structures in future explorations.

5 Conclusion

In this paper, we introduce AStar, an automated structured thinking paradigm for multimodal reasoning that effectively balances both performance and efficiency challenges in complex visual reasoning tasks. By introducing a lightweight library (*thought cards*) abstracted from 500 prior samples and adaptively retrieving problem-specific reasoning guidelines, our framework seamlessly integrates MLLMs’ internal capabilities with external explicit guidance. Extensive experiments demonstrate AStar’s remarkable results across multiple dimensions: achieving 53.9% accuracy on MathVerse and 32.7% on MathVision with only a 7B backbone, surpassing GPT-4o’s performance (50.2% and 30.4%). Further analysis across diverse tasks and model architectures confirms AStar’s generalizability and plug-and-play capability. Our findings suggest that AStar’s integration of structured decomposition with efficient prior guidance offers a promising pathway for advancing multimodal reasoning, making it more powerful and accessible to the broader research community.

References

- [1] Y. Wang, W. Chen, X. Han, X. Lin, H. Zhao, Y. Liu, B. Zhai, J. Yuan, Q. You, and H. Yang, “Exploring the reasoning abilities of multimodal large language models (mllms): A comprehensive survey on emerging trends in multimodal reasoning,” *arXiv preprint arXiv:2401.06805*, 2024.
- [2] OpenAI, “GPT-4o system card,” 2024.
- [3] R. Qiao, Q. Tan, G. Dong, M. Wu, C. Sun, X. Song, Z. GongQue, S. Lei, Z. Wei, M. Zhang, *et al.*, “We-math: Does your large multimodal model achieve human-like mathematical reasoning?,” *arXiv preprint arXiv:2407.01284*, 2024.
- [4] Z. Zhang, A. Zhang, M. Li, hai zhao, G. Karypis, and A. Smola, “Multimodal chain-of-thought reasoning in language models,” *Transactions on Machine Learning Research*, 2024.
- [5] K. Wang, J. Pan, W. Shi, Z. Lu, H. Ren, A. Zhou, M. Zhan, and H. Li, “Measuring multimodal mathematical reasoning with MATH-vision dataset,” in *The Thirty-eight Conference on Neural Information Processing Systems Datasets and Benchmarks Track*, 2024.
- [6] OpenAI, “Learning to reason with llms,” September 2024.
- [7] D. Guo, D. Yang, H. Zhang, J. Song, R. Zhang, R. Xu, Q. Zhu, S. Ma, P. Wang, X. Bi, *et al.*, “Deepseek-r1: Incentivizing reasoning capability in llms via reinforcement learning,” *arXiv preprint arXiv:2501.12948*, 2025.

- [8] K. Team, A. Du, B. Gao, B. Xing, C. Jiang, C. Chen, C. Li, C. Xiao, C. Du, C. Liao, *et al.*, “Kimi k1. 5: Scaling reinforcement learning with llms,” *arXiv preprint arXiv:2501.12599*, 2025.
- [9] J. Wei, X. Wang, D. Schuurmans, M. Bosma, F. Xia, E. Chi, Q. V. Le, D. Zhou, *et al.*, “Chain-of-thought prompting elicits reasoning in large language models,” *Advances in neural information processing systems*, vol. 35, pp. 24824–24837, 2022.
- [10] G. Xu, P. Jin, L. Hao, Y. Song, L. Sun, and L. Yuan, “Llava-o1: Let vision language models reason step-by-step,” *arXiv preprint arXiv:2411.10440*, 2024.
- [11] Y. Dong, Z. Liu, H.-L. Sun, J. Yang, W. Hu, Y. Rao, and Z. Liu, “Insight-v: Exploring long-chain visual reasoning with multimodal large language models,” *arXiv preprint arXiv:2411.14432*, 2024.
- [12] Y. Du, Z. Liu, Y. Li, W. X. Zhao, Y. Huo, B. Wang, W. Chen, Z. Liu, Z. Wang, and J.-R. Wen, “Virgo: A preliminary exploration on reproducing o1-like mllm,” *arXiv preprint arXiv:2501.01904*, 2025.
- [13] R. Luo, Z. Zheng, Y. Wang, Y. Yu, X. Ni, Z. Lin, J. Zeng, and Y. Yang, “Ursa: Understanding and verifying chain-of-thought reasoning in multimodal mathematics,” *arXiv preprint arXiv:2501.04686*, 2025.
- [14] G. Dong, C. Zhang, M. Deng, Y. Zhu, Z. Dou, and J.-R. Wen, “Progressive multimodal reasoning via active retrieval,” *arXiv preprint arXiv:2412.14835*, 2024.
- [15] H. Yao, J. Huang, W. Wu, J. Zhang, Y. Wang, S. Liu, Y. Wang, Y. Song, H. Feng, L. Shen, *et al.*, “Mulberry: Empowering mllm with o1-like reasoning and reflection via collective monte carlo tree search,” *arXiv preprint arXiv:2412.18319*, 2024.
- [16] Y. Wang, S. Wu, Y. Zhang, W. Wang, Z. Liu, J. Luo, and H. Fei, “Multimodal chain-of-thought reasoning: A comprehensive survey,” *arXiv preprint arXiv:2503.12605*, 2025.
- [17] Z. Shao, P. Wang, Q. Zhu, R. Xu, J. Song, X. Bi, H. Zhang, M. Zhang, Y. Li, Y. Wu, *et al.*, “Deepseekmath: Pushing the limits of mathematical reasoning in open language models,” *arXiv preprint arXiv:2402.03300*, 2024.
- [18] J. Zhang, J. Huang, H. Yao, S. Liu, X. Zhang, S. Lu, and D. Tao, “R1-vl: Learning to reason with multimodal large language models via step-wise group relative policy optimization,” *arXiv preprint arXiv:2503.12937*, 2025.
- [19] Y. Hu, W. Shi, X. Fu, D. Roth, M. Ostendorf, L. Zettlemoyer, N. A. Smith, and R. Krishna, “Visual sketchpad: Sketching as a visual chain of thought for multimodal language models,” *arXiv preprint arXiv:2406.09403*, 2024.
- [20] Y. Peng, G. Zhang, M. Zhang, Z. You, J. Liu, Q. Zhu, K. Yang, X. Xu, X. Geng, and X. Yang, “Lmm-r1: Empowering 3b llms with strong reasoning abilities through two-stage rule-based rl,” *arXiv preprint arXiv:2503.07536*, 2025.
- [21] Z. Liu, Y. Zhang, F. Liu, C. Zhang, Y. Sun, and J. Wang, “Othink-mr1: Stimulating multimodal generalized reasoning capabilities through dynamic reinforcement learning,” *arXiv preprint arXiv:2503.16081*, 2025.
- [22] Y. Yue, Z. Chen, R. Lu, A. Zhao, Z. Wang, S. Song, and G. Huang, “Does reinforcement learning really incentivize reasoning capacity in llms beyond the base model?,” *arXiv preprint arXiv:2504.13837*, 2025.
- [23] K. Gandhi, A. Chakravarthy, A. Singh, N. Lile, and N. D. Goodman, “Cognitive behaviors that enable self-improving reasoners, or, four habits of highly effective stars,” *arXiv preprint arXiv:2503.01307*, 2025.
- [24] P. I. Jaffe, R. A. Poldrack, R. J. Schafer, and *et al.*, “Modelling human behaviour in cognitive tasks with latent dynamical systems,” *Nature Human Behaviour*, vol. 7, pp. 986–1000, 2023.
- [25] D. Kahneman, *Thinking, Fast and Slow*. New York, NY: Farrar, Straus and Giroux, 2011.

- [26] S. Da Silva, “System 1 vs. system 2 thinking,” *Psych*, vol. 5, no. 4, pp. 1057–1076, 2023.
- [27] O. Thawakar, D. Dissanayake, K. More, R. Thawkar, A. Heakl, N. Ahsan, Y. Li, M. Zumri, J. Lahoud, R. M. Anwer, *et al.*, “Llamav-o1: Rethinking step-by-step visual reasoning in llms,” *arXiv preprint arXiv:2501.06186*, 2025.
- [28] L. Yang, Z. Yu, T. Zhang, S. Cao, M. Xu, W. Zhang, J. E. Gonzalez, and B. Cui, “Buffer of thoughts: Thought-augmented reasoning with large language models,” *Advances in Neural Information Processing Systems*, 2024.
- [29] S. Yin, C. Fu, S. Zhao, K. Li, X. Sun, T. Xu, and E. Chen, “A survey on multimodal large language models,” *arXiv preprint arXiv:2306.13549*, 2023.
- [30] L. Kocsis and C. Szepesvári, “Bandit based monte-carlo planning,” in *Machine Learning: ECML 2006* (J. Fürnkranz, T. Scheffer, and M. Spiliopoulou, eds.), (Berlin, Heidelberg), pp. 282–293, Springer Berlin Heidelberg, 2006.
- [31] S. Russell and E. Wefald, “Principles of metareasoning,” *Artificial Intelligence*, vol. 49, no. 1, pp. 361–395, 1991.
- [32] D. Roberts and L. Roberts, “Smart vision-language reasoners,” *arXiv preprint arXiv:2407.04212*, 2024.
- [33] F.-L. Lee and R. Heyworth, “Problem complexity: A measure of problem difficulty in algebra by using computer,” *Education Journal*, vol. 28, no. 1, pp. 85–108, 2000.
- [34] A. Radford, J. W. Kim, C. Hallacy, A. Ramesh, G. Goh, S. Agarwal, G. Sastry, A. Askell, P. Mishkin, J. Clark, *et al.*, “Learning transferable visual models from natural language supervision,” in *International conference on machine learning*, pp. 8748–8763, PmLR, 2021.
- [35] M. Muja and D. G. Lowe, “Scalable nearest neighbor algorithms for high dimensional data,” *IEEE Transactions on Pattern Analysis and Machine Intelligence*, vol. 36, no. 11, pp. 2227–2240, 2014.
- [36] P. Lu, H. Bansal, T. Xia, J. Liu, C. Li, H. Hajishirzi, H. Cheng, K.-W. Chang, M. Galley, and J. Gao, “Mathvista: Evaluating mathematical reasoning of foundation models in visual contexts,” *arXiv preprint arXiv:2310.02255*, 2023.
- [37] R. Zhang, D. Jiang, Y. Zhang, H. Lin, Z. Guo, P. Qiu, A. Zhou, P. Lu, K.-W. Chang, Y. Qiao, *et al.*, “Mathverse: Does your multi-modal llm truly see the diagrams in visual math problems?,” in *European Conference on Computer Vision*, pp. 169–186, Springer, 2025.
- [38] Y. Zong and X. Qiu, “GAOKAO-MM: A Chinese human-level benchmark for multimodal models evaluation,” in *Findings of the Association for Computational Linguistics: ACL 2024* (L.-W. Ku, A. Martins, and V. Srikumar, eds.), (Bangkok, Thailand), pp. 8817–8825, Association for Computational Linguistics, Aug. 2024.
- [39] A. Masry, X. L. Do, J. Q. Tan, S. Joty, and E. Hoque, “ChartQA: A benchmark for question answering about charts with visual and logical reasoning,” in *Findings of the Association for Computational Linguistics: ACL 2022* (S. Muresan, P. Nakov, and A. Villavicencio, eds.), (Dublin, Ireland), pp. 2263–2279, Association for Computational Linguistics, May 2022.
- [40] L. Chen, J. Li, X. Dong, P. Zhang, Y. Zang, Z. Chen, H. Duan, J. Wang, Y. Qiao, D. Lin, and F. Zhao, “Are we on the right way for evaluating large vision-language models?,” in *The Thirty-eighth Annual Conference on Neural Information Processing Systems*, 2024.
- [41] X. Yue, Y. Ni, K. Zhang, T. Zheng, R. Liu, G. Zhang, S. Stevens, D. Jiang, W. Ren, Y. Sun, C. Wei, B. Yu, R. Yuan, R. Sun, M. Yin, B. Zheng, Z. Yang, Y. Liu, W. Huang, H. Sun, Y. Su, and W. Chen, “Mmmu: A massive multi-discipline multimodal understanding and reasoning benchmark for expert agi,” in *Proceedings of CVPR*, 2024.
- [42] X. Fu, Y. Hu, B. Li, Y. Feng, H. Wang, X. Lin, D. Roth, N. A. Smith, W.-C. Ma, and R. Krishna, “Blink: Multimodal large language models can see but not perceive,” in *Computer Vision – ECCV 2024* (A. Leonardis, E. Ricci, S. Roth, O. Russakovsky, T. Sattler, and G. Varol, eds.), (Cham), pp. 148–166, Springer Nature Switzerland, 2025.

- [43] Qwen Team, “Qwen2.5: A party of foundation models,” September 2024.
- [44] S. Bai, K. Chen, X. Liu, J. Wang, W. Ge, S. Song, K. Dang, P. Wang, S. Wang, J. Tang, *et al.*, “Qwen2. 5-vl technical report,” *arXiv preprint arXiv:2502.13923*, 2025.
- [45] P. Wang, S. Bai, S. Tan, S. Wang, Z. Fan, J. Bai, K. Chen, X. Liu, J. Wang, W. Ge, *et al.*, “Qwen2-vl: Enhancing vision-language model’s perception of the world at any resolution,” *arXiv preprint arXiv:2409.12191*, 2024.
- [46] Z. Chen, J. Wu, W. Wang, W. Su, G. Chen, S. Xing, M. Zhong, Q. Zhang, X. Zhu, L. Lu, *et al.*, “Internvl: Scaling up vision foundation models and aligning for generic visual-linguistic tasks,” in *Proceedings of the IEEE/CVF Conference on Computer Vision and Pattern Recognition*, pp. 24185–24198, 2024.
- [47] W. Shi, Z. Hu, Y. Bin, J. Liu, Y. Yang, S.-K. Ng, L. Bing, and R. K.-W. Lee, “Math-LLaVA: Bootstrapping mathematical reasoning for multimodal large language models,” in *Findings of the Association for Computational Linguistics: EMNLP 2024*, (Miami, Florida, USA), pp. 4663–4680, Association for Computational Linguistics, Nov. 2024.
- [48] F. Meng, L. Du, Z. Liu, Z. Zhou, Q. Lu, D. Fu, T. Han, B. Shi, W. Wang, J. He, *et al.*, “Mm-eureka: Exploring the frontiers of multimodal reasoning with rule-based reinforcement learning,” *arXiv preprint arXiv:2503.07365*, 2025.
- [49] OpenAI, “GPT-4V(ision) system card,” 2023.
- [50] D. Zhu, J. Chen, X. Shen, X. Li, and M. Elhoseiny, “Minigt-4: Enhancing vision-language understanding with advanced large language models,” *arXiv preprint arXiv:2304.10592*, 2023.
- [51] H. Liu, C. Li, Y. Li, and Y. J. Lee, “Improved baselines with visual instruction tuning,” in *Proceedings of the IEEE/CVF Conference on Computer Vision and Pattern Recognition*, pp. 26296–26306, 2024.
- [52] Z. Lin, C. Liu, R. Zhang, P. Gao, L. Qiu, H. Xiao, H. Qiu, C. Lin, W. Shao, K. Chen, *et al.*, “Sphinx: The joint mixing of weights, tasks, and visual embeddings for multi-modal large language models,” *arXiv preprint arXiv:2311.07575*, 2023.
- [53] H. Liu, C. Li, Y. Li, B. Li, Y. Zhang, S. Shen, and Y. J. Lee, “Llava-next: Improved reasoning, ocr, and world knowledge,” 2024.
- [54] X. Dong, P. Zhang, Y. Zang, Y. Cao, B. Wang, L. Ouyang, X. Wei, S. Zhang, H. Duan, M. Cao, *et al.*, “Internlm-xcomposer2: Mastering free-form text-image composition and comprehension in vision-language large model,” *arXiv preprint arXiv:2401.16420*, 2024.
- [55] H. Lu, W. Liu, B. Zhang, B. Wang, K. Dong, B. Liu, J. Sun, T. Ren, Z. Li, H. Yang, *et al.*, “Deepseek-vl: towards real-world vision-language understanding,” *arXiv preprint arXiv:2403.05525*, 2024.
- [56] J. Gao, R. Pi, J. Zhang, J. Ye, W. Zhong, Y. Wang, L. Hong, J. Han, H. Xu, Z. Li, *et al.*, “G-llava: Solving geometric problem with multi-modal large language model,” *arXiv preprint arXiv:2312.11370*, 2023.
- [57] W. Zhuang, X. Huang, X. Zhang, and J. Zeng, “Math-puma: Progressive upward multimodal alignment to enhance mathematical reasoning,” *arXiv preprint arXiv:2408.08640*, 2024.
- [58] R. Zhang, X. Wei, D. Jiang, Z. Guo, S. Li, Y. Zhang, C. Tong, J. Liu, A. Zhou, B. Wei, *et al.*, “Mavis: Mathematical visual instruction tuning with an automatic data engine,” *arXiv preprint arXiv:2407.08739*, 2024.
- [59] X. Han, Y. Jian, X. Hu, H. Liu, Y. Wang, Q. Fan, Y. Ai, H. Huang, R. He, Z. Yang, *et al.*, “Infimm-webmath-40b: Advancing multimodal pre-training for enhanced mathematical reasoning,” in *The 4th Workshop on Mathematical Reasoning and AI at NeurIPS’24*, 2024.
- [60] S. Peng, D. Fu, L. Gao, X. Zhong, H. Fu, and Z. Tang, “Multimath: Bridging visual and mathematical reasoning for large language models,” *arXiv preprint arXiv:2409.00147*, 2024.

- [61] X. Zhang, J. Li, W. Chu, J. Hai, R. Xu, Y. Yang, S. Guan, J. Xu, and P. Cui, “On the out-of-distribution generalization of multimodal large language models,” *arXiv preprint arXiv:2402.06599*, 2024.
- [62] H. Dong, Y. Zhao, E. Chatzi, and O. Fink, “MultiOOD: Scaling out-of-distribution detection for multiple modalities,” in *The Thirty-eighth Annual Conference on Neural Information Processing Systems*, 2024.
- [63] J. Chen, S. Xiao, P. Zhang, K. Luo, D. Lian, and Z. Liu, “BGE m3-embedding: Multi-lingual, multi-functionality, multi-granularity text embeddings through self-knowledge distillation,” *CoRR*, vol. abs/2402.03216, 2024.
- [64] M. Ester, H. Kriegel, J. Sander, and X. Xu, “A density-based algorithm for discovering clusters in large spatial databases with noise,” in *Proceedings of the Second International Conference on Knowledge Discovery and Data Mining (KDD-96), Portland, Oregon, USA* (E. Simoudis, J. Han, and U. M. Fayyad, eds.), pp. 226–231, AAAI Press, 1996.
- [65] W. Wang, Z. Chen, W. Wang, Y. Cao, Y. Liu, Z. Gao, J. Zhu, X. Zhu, L. Lu, Y. Qiao, *et al.*, “Enhancing the reasoning ability of multimodal large language models via mixed preference optimization,” *arXiv preprint arXiv:2411.10442*, 2024.
- [66] Z. Qi, M. Ma, J. Xu, L. L. Zhang, F. Yang, and M. Yang, “Mutual reasoning makes smaller llms stronger problem-solvers,” *arXiv preprint arXiv:2408.06195*, 2024.
- [67] J. Wu, M. Feng, S. Zhang, F. Che, Z. Wen, and J. Tao, “Beyond examples: High-level automated reasoning paradigm in in-context learning via mcts,” *arXiv preprint arXiv:2411.18478*, 2024.
- [68] C. Cui, Y. Ma, X. Cao, W. Ye, Y. Zhou, K. Liang, J. Chen, J. Lu, Z. Yang, K.-D. Liao, *et al.*, “A survey on multimodal large language models for autonomous driving,” in *Proceedings of the IEEE/CVF Winter Conference on Applications of Computer Vision*, pp. 958–979, 2024.
- [69] P. Wang, L. Li, Z. Shao, R. Xu, D. Dai, Y. Li, D. Chen, Y. Wu, and Z. Sui, “Math-shepherd: Verify and reinforce LLMs step-by-step without human annotations,” in *Proceedings of the 62nd Annual Meeting of the Association for Computational Linguistics (Volume 1: Long Papers)* (L.-W. Ku, A. Martins, and V. Srikumar, eds.), (Bangkok, Thailand), pp. 9426–9439, Association for Computational Linguistics, Aug. 2024.
- [70] S. Yao, D. Yu, J. Zhao, I. Shafran, T. Griffiths, Y. Cao, and K. Narasimhan, “Tree of thoughts: Deliberate problem solving with large language models,” in *Advances in Neural Information Processing Systems* (A. Oh, T. Naumann, A. Globerson, K. Saenko, M. Hardt, and S. Levine, eds.), vol. 36, pp. 11809–11822, Curran Associates, Inc., 2023.
- [71] S. Hao, Y. Gu, H. Ma, J. Hong, Z. Wang, D. Wang, and Z. Hu, “Reasoning with language model is planning with world model,” in *Proceedings of the 2023 Conference on Empirical Methods in Natural Language Processing* (H. Bouamor, J. Pino, and K. Bali, eds.), (Singapore), pp. 8154–8173, Association for Computational Linguistics, Dec. 2023.
- [72] S. Wu, Z. Peng, X. Du, T. Zheng, M. Liu, J. Wu, J. Ma, Y. Li, J. Yang, W. Zhou, *et al.*, “A comparative study on reasoning patterns of openai’s o1 model,” *arXiv preprint arXiv:2410.13639*, 2024.
- [73] G. Team, R. Anil, S. Borgeaud, J.-B. Alayrac, J. Yu, R. Soricut, J. Schalkwyk, A. M. Dai, A. Hauth, K. Millican, *et al.*, “Gemini: a family of highly capable multimodal models,” *arXiv preprint arXiv:2312.11805*, 2023.
- [74] J. Bai, S. Bai, S. Yang, S. Wang, S. Tan, P. Wang, J. Lin, C. Zhou, and J. Zhou, “Qwen-vl: A versatile vision-language model for understanding, localization, text reading, and beyond,” *arXiv preprint arXiv:2308.12966*, vol. 1, no. 2, p. 3, 2023.
- [75] Anthropic, “Introducing the next generation of claude,” March 2024.
- [76] Y. Yang, Y. Ma, and P. Liu, “Weak-to-strong reasoning,” in *Findings of the Association for Computational Linguistics: EMNLP 2024* (Y. Al-Onaizan, M. Bansal, and Y.-N. Chen, eds.), (Miami, Florida, USA), pp. 8350–8367, Association for Computational Linguistics, Nov. 2024.

- [77] S. Kotz and N. L. Johnson, eds., *Breakthroughs in Statistics: Methodology and Distribution*. New York, NY: Springer New York, 1992.

Appendix of AStar

This comprehensive supplementary material provides in-depth insights into our AStar method, covering additional descriptions, experimental details, and results. The appendix is organized as follows:

Contents

A. TL;DR: Main Contributions and Takeaways

B. Preliminaries

- B.1. Overall Notations
- B.2. MLLM Reasoning
- B.3. Monte Carlo Tree Search
- B.4. Verification Methods (Self-Consistency and Outcome Reward Model)

C. Algorithm Details

- C.1. Action Space
- C.2. Reward Value in MCTS

D. Detailed Experimental Setup

- D.1. Benchmarks and Datasets
- D.2. Comparison Baselines
- D.3. Implementation Details

E. Supplementary Results

- E.1. Detailed Results on Multimodal Reasoning Benchmarks
- E.2. Comparison with Strong Baselines
- E.3. Weak-to-Strong Generalization
- E.4. Statistical Validation

F. Case Study

G. Further Discussions

A TL;DR: Main Contributions and Takeaways

Takeaways

1. External reasoning guidelines unlock latent capabilities in resource-efficient models, effectively bridging the performance gap with significantly larger architectures. (**Figure 1,4**).
2. The universality of high-level thought patterns transcends specific tasks, domains, and modalities, suggesting fundamental cognitive principles that generalize across diverse problem spaces (§3.2).
3. Minimal data requirements (500 samples) demonstrate the power of explicit pattern extraction over large-scale implicit learning approaches (§3.3).
4. AStar’s modular design enables seamless integration with post-training techniques like GRPO, creating complementary performance gains without requiring architectural modifications (**Figure 7**).

In this work, we focus on exploring how to enhance MLLMs’ complex visual reasoning capabilities that demand both visual perception and high-level cognition. While mainstream multimodal reasoning approaches typically rely on computationally intensive explicit search mechanisms or post-training procedures requiring substantial data and computational resources, no prior work has sufficiently explored combining external reasoning patterns with internal capabilities to improve both efficiency and effectiveness. To bridge this gap, we present AStar, a novel thought-augmented reasoning framework with the following contributions:

- **Novel Reasoning Paradigm:** We introduce “*thought cards*”, a lightweight library of high-level reasoning patterns abstracted from just 500 prior examples. This training-free framework effectively bridges the gap between search-based and post-training methods, offering both performance enhancement and computational efficiency.
- **Effectiveness and Efficiency:** AStar achieves superior results on challenging benchmarks using only a 7B-parameter backbone model, surpassing GPT-4o on MathVerse (53.9% vs. 50.2%) and MathVision (32.7% vs. 30.4%), highlighting exceptional resource efficiency.
- **Broad Generalization Capability:** Our framework demonstrates remarkable versatility across diverse tasks, domains, and modalities, validating the universality of high-level problem-solving thoughts across different problem spaces.
- **Plug-and-Play Flexibility:** AStar’s modular design allows seamless integration with existing post-training strategies like GRPO, enhancing their capabilities without requiring structural modifications—particularly valuable in resource-constrained environments.

By introducing generalizable external reasoning guidelines that complement models’ internal capabilities, our approach provides a practical and scalable solution for enhancing multimodal reasoning capabilities even with limited computational resources. We anticipate that our findings will stimulate further exploration into the integration of explicit cognitive frameworks with MLLMs, advancing both theoretical understanding and practical applications across diverse domains.

B Preliminaries

This section describes Overall Notations (B.1), MLLM Reasoning (B.2), Monte Carlo Tree Search (B.3), and Verification Methods (Self-Consistency and Outcome Reward Model) (B.4).

B.1 Overall Notations

The definitions for notations are in Table 5.

Table 5: Notation Table

Character	Meaning
π_θ	policy MLLM
I	task instruction
\mathcal{D}_I	demonstration examples of I , which is ϕ in zero-shot settings
D_s	seed data
D_t	test data
x_t	multimodal test problem, consisting of input question q and images i
y_d	
y_g	decoded answer
y_t	gold standard answer
T	reasoning trajectory / solution
T_d	number of reasoning steps
a_t	number of tokens in decoded answer y_p
s_t	t-th decoded answer token of y_d
S_t	t-th reasoning step of trajectory y_t
a_t	t-th state, which consists of input x and preceding reasoning steps $(s_1, s_2, \dots, s_{t-1})$
s	t-th action based on the previous state S_{t-1}
p	node s in the tree structure
$Q(s)$	parent node of s
p_φ	reward value of node s
o_ψ	process reward model
	outcome reward model

B.2 MLLM Reasoning

With the advancement of computational resources and expanded datasets, MLLMs have demonstrated remarkable capabilities across various multimodal tasks [29, 1]. These range from visual reasoning tasks like chart understanding and visual question-answering [39] to more complex perception-action tasks in autonomous driving and robotics [68], where models must integrate visual inputs with decision-making processes. Central to these achievements is the development of effective reasoning methods, which can substantially enhance MLLM problem-solving capabilities, enabling even smaller models to achieve sophisticated reasoning abilities [45, 14, 27]. To formalize this reasoning process, we consider an autoregressive pre-trained MLLM serving as a policy model π_θ . Given an input problem x_t , the model generates a sequence $output = (s_0, s_1, s_2, \dots, s_T)$ through iterative token prediction, where $s_0 := x_t$ represents the initial state and s_T corresponds to the solution y_p . We define this generated sequence $(s_0, s_1, s_2, \dots, s_T)$ as a reasoning trajectory y_t . The conditional probability distribution of generating the complete reasoning trajectory is:

$$\pi_\theta(y_t, y_d \mid I, x_t, \mathcal{D}_I) = \underbrace{\prod_{t=1}^T \pi_\theta(s_t \mid s_{<t}, I, x_t, \mathcal{D}_I)}_{\text{Intermediate Reasoning Process}} \cdot \underbrace{\prod_{t=1}^{T_d} \pi_\theta(a'_t \mid a'_{<t}, y_t, I, x_t)}_{\text{Answer Decoding}}, \quad (13)$$

Following previous studies, we can conceptualize MLLMs as world models, with the complex reasoning process formulated as a Markov decision process. Specifically, when addressing complex reasoning challenges in real-world scenarios, at each time step t , the model receives a state S_{t-1} , comprising the original input problem x and preceding reasoning steps $(s_0, s_1, s_2, \dots, s_{t-1})$. The policy model π_θ then generates the current action $a_t = \pi_\theta(\Phi(S_{t-1}))$, which prompts the MLLM to produce the next reasoning step s_t . The entire process, from the initial step s_0 to the final output s_T , naturally forms a complete trajectory or chain of thought.

Inspired by recent advances in language model reasoning capabilities, researchers have explored OpenAI o1-like structured reasoning approaches to enhance long-chain reasoning in MLLMs. These approaches aim to develop systematic thinking patterns that enable models to perform complex multi-step reasoning. The process can be formalized under the following theoretical framework:

$$P_{\pi_\theta}(y_d = y_g \mid x_t) = \mathbb{E}_{(s_0, s_1, \dots, s_T) \sim P_{\pi_\theta}(y_t \mid x_t)} [P(y_d = y_g \mid s_0, s_1, \dots, s_T, x_t)] \quad (14)$$

Table 6: Comparison with two primary reasoning methods: search-based methods (AR-MCTS, Mulberry) and post-training methods (SFT: LLaVA-CoT, LlamaV-o1, URSA; GRPO: LMM-R1, MM-Eureka, R1-VL). ‘OS Only’ indicates datasets constructed only with open-source models. AStar only requires 500 prior samples.

Method	Type	Open-Source Only	Training-Free	Training Data	Training Cost ↓	Inference Cost ↓
AR-MCTS [14]	Search	✓	✓	34.5K	-	High
Mulberry [15]	Search	✗	✗	260K	High	Low
LLaVA-CoT [10]	SFT	✗	✗	100K	High	Low
LlamaV-o1 [27]	SFT	✗	✗	118K	High	Low
URSA [13]	SFT	✗	✗	1100K	High	Low
LMM-R1-3B [20]	GRPO	✓	✗	55.3K	High	Low
MM-Eureka-7B [48]	GRPO	✓	✗	15K	High	Low
R1-VL-7B [18]	GRPO	✓	✗	260K	High	Low
AStar (Ours)	-	✓	✓	0.5K	Low	Low

where $P(y_d = y_g \mid s_0, s_1, \dots, s_T, x)$ represents the probability of obtaining an accurate final answer given the test problem x_t and reasoning trajectory y_t .

Early work explored multimodal chain-of-thought (CoT) [4], addressing the limitations of conventional MLLMs that typically defaulted to a simple “direct prediction” mode due to the scarcity of high-quality long-chain reasoning data. However, these approaches often exhibit instability in multimodal reasoning tasks due to the distribution shift between training and inference. Two primary methods have emerged to address this challenge: *explicit search mechanisms* and *post-training methods*. Recent advances are summarized in Table 6.

(1) *Explicit search mechanisms*. These approaches leverage explicit search structures (e.g., Monte Carlo tree search, MCTS) with specialized reward models to guide the exploration of solution paths. AR-MCTS [14] combines MCTS with active retrieval to expand the solution space and enhance performance, though its extensive iterations demand significant computational resources. Moreover, the quality and relevance of retrieved examples at each exploration step substantially impact model performance. Similarly, Mulberry [15] employs collective knowledge to enable collaborative conjecture, search, and identification of effective reasoning paths via MCTS. However, it requires substantial training data (260K samples) generated with expensive proprietary models, making it computationally intensive.

(2) *Post-Training Methods*. This approach focus on developing structured reasoning capabilities through techniques such as Supervised Fine-Tuning (SFT) or Reinforcement Learning with Verifiable Rewards (RLVR). SFT-based approaches like LLaVA-CoT [10] and URSA [13] distill structured reasoning patterns through long-form CoT data, typically requiring substantial training data ($\geq 100K$ samples) and supervision from proprietary models. RLVR-based methods like LMM-R1 [20] and R1-VL [18] leverage techniques such as Group Relative Policy Optimization (GRPO) [17, 18], but encounter challenges with exploration depth and training stability. As shown in [22, 23], these methods primarily function by biasing the model’s output distribution toward reward-maximizing paths without introducing external knowledge, inherently limiting their exploration capacity.

B.3 Monte Carlo Tree Search

Leveraging Monte Carlo Tree Search (MCTS), recent approaches like AR-MCTS [14] exploit MLLMs’ intrinsic capabilities and active retrieval for iterative exploration to enhance visual complex reasoning. However, these methods demand substantial computational resources due to extensive iterations. While approaches like Mulberry [15] attempt to integrate tree structures through model training, they require large-scale datasets and significant computational overhead. Moreover, current methods typically employ static reasoning processes, lacking the ability to adapt reasoning strategies based on problem complexity. In contrast, our approach employs MCTS only during the generation of prior reasoning patterns (referred to as “thought cards” in Sec. 2.2) and references these thought cards during inference to achieve efficient reasoning. This design enables AStar to adaptively match reasoning strategies to problem attributes, significantly reducing time complexity compared to traditional explicit search methods while maintaining comprehensive search coverage and performance. Furthermore, compared to traditional MCTS, we implement two key improvements in our card generation process to achieve efficient MCTS operations: (1) We introduce early termination strategies

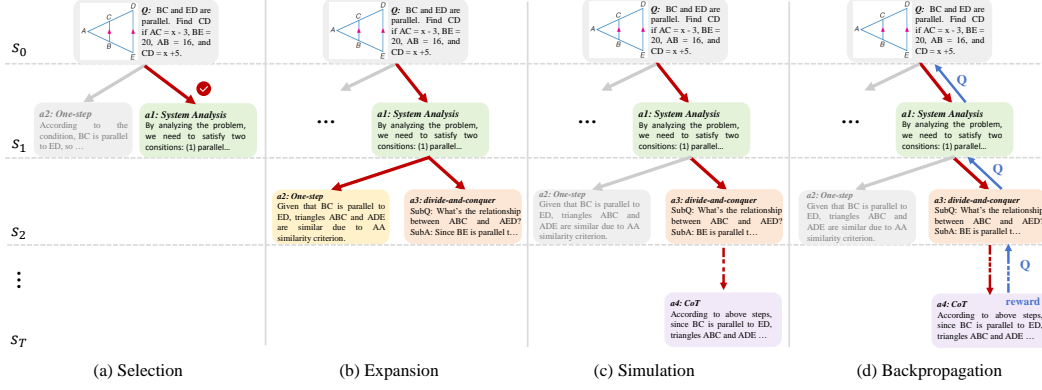


Figure 10: An illustration of the four phases in an iteration of MCTS for complex reasoning tasks.

and integrate the MLLM’s reasoning process during MCTS iteration; (2) We use the likelihood of self-consistency majority voting as the reward value, enabling supervision-free generalization.

B.4 Verification Methods (Self-Consistency and Outcome Reward Model)

After obtaining multiple valid candidate solutions for the test multimodal query $x_t = [q; i]$, selecting the most accurate reasoning trajectory among candidates presents a critical challenge. In multimodal reasoning, self-consistency represents a simple yet effective approach, where the final answer is determined through majority voting among sampled paths:

$$y^* = \arg \max_{y \in Y} \sum_{i=1}^m \mathbb{I}(y_i = y) \quad (15)$$

where Y denotes the set of all possible decoded answers, and \mathbb{I} is the indicator function. This strategy exploits the observation that a complex reasoning problem typically admits multiple valid reasoning paths leading to its unique correct answer. Thus, repeatedly sampled actions at the same state likely indicate successful task completion. However, for complex reasoning tasks where models may only achieve correct reasoning with low probability, simple self-consistency might not provide stable performance.

Recent advances in LLM reasoning verification have demonstrated significant improvements in reasoning capabilities through verification modules [67]. This has motivated the integration of outcome and process supervision in multimodal domains [14, 13] to enhance reasoning performance. However, the scarcity of multimodal supervision data and challenges in ensuring supervision signal quality often compromise verification effectiveness, with few high-performance open-source verification models currently available. Therefore, for simplicity, we leverage mature text-domain outcome reward models (ORM).

Specifically, in the text domain, given a text problem q and its reasoning trajectory y_t , ORM ($\mathcal{D} \times \mathcal{S} \rightarrow \mathbb{R}$) assigns a single real-value to indicate whether y_t is correct. ORM is usually trained with a cross-entropy loss:

$$\mathcal{L}_{\text{ORM}} = y_g \log r_{y_t} + (1 - y_g) \log(1 - r_{y_t}) \quad (16)$$

where y_g is the golden answer ($y_g = 1$ if $traj$ is correct else $y_g = 0$), and r_{traj} is the sigmoid score of $traj$ assigned by ORM. The effectiveness of ORM heavily depends on training data quality. For reasoning problems with definitive answers, researchers can construct the ORM training set automatically by: (1) sampling candidate solutions, and (2) labeling solutions based on answer correctness. While this approach may introduce false positives (incorrect reasoning leading to correct answers), prior work has demonstrated its effectiveness in training robust ORM models [69]. This enables the development of high-performing open-source verification models in the text domain.

To leverage these powerful text-domain verification models for visual reasoning while maintaining our principle of balancing performance and efficiency, we first use an MLLM (e.g., Qwen2-VL-7B)

to convert the visual input into a textual description, which is then combined with the original text query to form a pure-text question:

$$q = \pi_{\theta}(x_t, \text{prompt}_{\text{translate}}) \quad (17)$$

where $\text{prompt}_{\text{translate}}$ denotes a translation prompt (e.g., “please translate the question and visual image into a pure text format”). **This, along with the reasoning steps derived from AStar, is passed to the above ORM for evaluation. The top-3 highest-scoring paths are subsequently verified via self-consistency.**

Note that, this process does not leak any heuristics towards specific tasks. The verification mechanism operates independently from the problem-solving process, maintaining task-agnosticity. The ORM evaluates solution quality based on general reasoning principles rather than task-specific shortcuts. Our experiments indicate that this approach achieves improvements over simple self-consistency with minimal computational overhead. Future work could explore integration with high-quality verification models for potentially better results. In this paper, we utilize off-the-shelf ORM model: Llama3.1-8B-ORM-Mistral-Data².

Table 7: Comparison with other search-based LLM and MLLM methods. Note that, most methods contain limited space. In contrast, we define a rich set of reasoning actions, thus enhancing the upper bound of model reasoning capabilities.

Type	Method	Action Space
LLM	Tree-of-Thought [70]	a_3 : one-step thought
	RAP [71]	a_5 : divide and conquer
MLLM	AR-MCTS [14]	a_3 : one-step thought
	LLaVA-CoT [10]	a_4 : chain-of-thought
	URSA [13]	a_4 : chain-of-thought
	Ours	$a_1, a_2, a_3, a_4, a_5, a_6$

C Algorithm Details

C.1 Action Space

Reasoning capabilities are fundamental for handling diverse tasks, encompassing multiple cognitive dimensions. Prior work has categorized reasoning into deductive, inductive, abductive, and analogical approaches [1]. While open-source MLLMs demonstrate basic task competency, advanced models necessitate more sophisticated human-like reasoning abilities to achieve their full potential. A key insight from recent studies suggests that model reasoning performance is bounded by their available reasoning actions [72]. Current frameworks, however, operate within a constrained action space (Table 7), which may limit the reasoning capabilities of MLLMs. To expand models’ reasoning capabilities beyond these constraints, we propose a comprehensive framework with six fundamental reasoning actions:

- *Visual Parsing* (a_1): Specifically designed for visual reasoning, aimed at extracting and analyzing visual information to enable the model to **integrate visual cues with textual reasoning**
- *System Analysis* (a_2): Incorporates **complete image information** and combines textual queries with image data to analyze task conditions and constraints
- *One-Step Thought* (a_3): Generates the next one-step thought based on the given question (text and image information) and preceding reasoning steps.
- *Chain-of-Thought* (a_4): Facilitating step-by-step reasoning by constructing a logical sequence of intermediate thoughts, where each step incrementally builds on the previous ones.

²<https://huggingface.co/RLHFlow/Llama3.1-8B-ORM-Mistral-Data>

- *Divide and Conquer* (a_5): Breaking down a complex visual reasoning problem into several smaller subproblems and progressively solving them to achieve the overall solution.
- *Self-Reflection* (a_6): Engages in timely reflection of prior solutions according to **text and image sub-regions**, and implements necessary refinement during the reasoning process to ensure accuracy.

C.2 Reward Value in MCTS

To simplify the construction of thought cards via the MCTS iteration, we avoid introducing an external reward model to score each step. Given the current skepticism regarding the self-rewarding capabilities of language models, alternative methods are necessary. Inspired by the principle that actions leading to correct answers should be rewarded more frequently, we aim to increase their likelihood of selection in future MCTS tree expansions. Following prior work [66], we define the reward value as the likelihood of self-consistency via majority voting. Note that this principle applies only to leaf nodes. The Q-values of intermediate nodes are initially set to 0 and are dynamically updated during the backpropagation process, as described in Equation 1.

Table 8: The statistics of benchmarks used in this paper. Our evaluation encompasses three tasks: Visual Perception and Understanding (ChartQA, MMStar, MMMU, BLINK), Mathematical Reasoning (MathVista, MathVerse, MathVision), and Commonsense and Scientific Reasoning (GAOKAO-MM).

Type	Dataset	Evaluation Dimensions
Visual Perception and Understanding	ChartQA [39]	chart understanding and reasoning
	MMStar [40]	6 core capabilities, like scientific reasoning
	MMMU [41]	30 subjects and 183 subfields, like Art and Business
	BLINK [42]	14 visual perception tasks, like visual correspondence
Mathematical Reasoning	MathVista [36]	12 core capabilities, like arithmetic reasoning
	MathVerse [37]	6 distinct vision-text-dominant
	MathVision [5]	16 mathematical domains
Commonsense and Scientific Reasoning	GAOKAO-MM [38]	8 subjects, like history and Geography

D Detailed Experimental Setup

D.1 Benchmarks and Datasets

Here are the details of the benchmarks used in our experiments. The statistics of the datasets are recorded in Table 8. Note that the evaluation metrics for all datasets are consistent with their official standards, primarily focusing on accuracy.

- **ChartQA** [39] is a comprehensive benchmark for chart-based question answering that emphasizes visual and logical reasoning capabilities. The dataset comprises 9,608 human-authored questions and 23,111 machine-generated questions derived from human-written chart summaries. It incorporates 20,882 real-world charts from diverse sources including Statista, Pew Research, Our World in Data, and OECD, spanning multiple domains and visualization styles. ChartQA addresses prior dataset limitations through its focus on human-authored questions, real-world charts, and open-vocabulary responses. We utilize this dataset to evaluate our method’s performance on visual chart question-answering tasks commonly encountered in real-world scenarios.
- **MMStar** [40] serves as a vision-critical multimodal benchmark for evaluating MLLM capabilities. It addresses two fundamental limitations in existing evaluations: the redundancy of visual inputs and potential training data contamination. Comprising 1,500 meticulously curated challenge samples across six core competencies and 18 evaluation axes, the benchmark undergoes rigorous validation to ensure visual necessity and minimal data leakage. We employ this comprehensive dataset to assess our method’s general reasoning capabilities.
- **MMMU** [41] comprises 11,500 meticulously collected multimodal questions from college exams, quizzes, and textbooks, covering six core disciplines: Art & Design, Business, Science, Health & Medicine, Humanities & Social Science, and Tech & Engineering. These questions

span 30 subjects and 183 subfields, incorporating 30 highly heterogeneous image types such as charts, diagrams, maps, tables, music sheets, and chemical structures. Unlike existing benchmarks, MMMU focuses on multi-discipline multimodal understanding with domain-specific knowledge, challenging models to perform tasks akin to those faced by experts. Given the interleaved image-text format of the examples and disciplines, these capabilities are considered a kind of Interleaved Image-Text Understanding. We utilize this dataset to assess our method’s performance across a broad spectrum of real-world, expert-level visual perception and understanding.

- **BLINK** [42] is a benchmark that evaluates multimodal large language models (MLLMs) on core visual perception abilities not commonly assessed in other evaluations. It reformats 14 classic computer vision tasks into 3,807 multiple-choice questions, each paired with single or multiple images and visual prompts. Tasks include relative depth estimation, visual correspondence, forensics detection, and multi-view reasoning.
- **MathVista** [36] is a mathematical visual benchmark consisting of 6,141 examples. These examples are divided into two subsets: *testmini* with 1,000 annotated examples and *test* comprising 5,141 problems without public answers. We conduct our evaluation on the *testmini* subset to assess visual comprehension and compositional reasoning capabilities.
- **MathVerse** [37] is a comprehensive and specialized visual mathematics benchmark for assessing multimodal mathematical reasoning capabilities of MLLMs. The benchmark contains 2,612 visual math problems, combining 1,236 newly collected problems from public repositories with 1,376 problems from existing benchmarks. Human annotators have transformed each problem into six distinct versions—text-dominant, text-lite, text-only, vision-intensive, vision-dominant, and vision-only—each offering different levels of multimodal information. To ensure a fair comparison, we conduct evaluations on the *testmini* set of MathVerse, and construct seed data from the non-overlapping portion of the test set. Note that, MathVerse has no intersection with other tested benchmarks (e.g., GAOKAO-MM), thus preventing data leakage. We utilize this dataset to evaluate AStar’s performance across varying degrees of multimodal integration.
- **MathVision** [5] constitutes a meticulously compiled collection of 3,040 mathematics problems, each incorporating visual elements from authentic mathematics competitions. The dataset spans 16 mathematical domains and features a five-tier difficulty classification system. We employ this dataset to evaluate our model’s performance on challenging reasoning tasks.
- **GAOKAO-MM** [38] represents a multimodal evaluation framework derived from the Chinese National College Entrance Examination (Gaokao). It encompasses eight academic subjects and includes twelve categories of images, such as diagrams, function graphs, maps, and photographs. The benchmark aims to evaluate models’ abilities to understand and reason over diverse multimodal content, reflecting the complexity and breadth of knowledge. We leverage this dataset to assess AStar’s cross-domain generalization capabilities.

D.2 Comparison Baselines

We evaluate AStar against four strong baseline categories:

Open-source general MLLMs: Recent advances include Qwen2-VL [45] and InternVL2 [46], which demonstrate exceptional capabilities in complex reasoning and mathematical problem-solving.

Open-source math MLLMs: Several models have been specifically optimized for mathematical reasoning in MLLMs. These models can be grouped based on their core methodologies:

1. Dataset Construction and Fine-Tuning:

- a. **G-LLaVA** [56]: Introduces the Geo170K dataset, comprising over 170K geometric image-caption and question-answer pairs, to enhance MLLMs’ geometric problem-solving capabilities.
- b. **Math-LLaVA** [47]: Develops the MathV360K dataset by collecting 40K high-quality images with question-answer pairs and synthesizing an additional 320K pairs, then fine-tunes the LLaVA-1.5 model to improve multimodal mathematical reasoning.
- c. **MultiMath** [60]: Constructs the MultiMath-300K dataset, encompassing K-12 level mathematical problems with image captions and step-wise solutions, and trains the MultiMath-7B model to bridge visual and mathematical reasoning.

2. *Progressive Alignment and Curriculum Learning:*

- a. Math-PUMA [57]: Proposes a three-stage Progressive Upward Multimodal Alignment methodology to enhance MLLMs’ mathematical reasoning skills, focusing on aligning visual and textual modalities through a structured training process.
- b. LlamaV-o1 [27]: Introduces a multimodal visual reasoning model trained using a multi-step curriculum learning approach, organizing tasks progressively to facilitate incremental skill acquisition and problem-solving.

3. *CoT Reasoning Integration:*

- a. LLaVA-CoT [10]: Develops a vision-language model designed to conduct autonomous multi-stage reasoning, employing a structured approach that includes summarization, visual interpretation, logical reasoning, and conclusion generation.
- b. URSA [13]: Proposes a three-module synthesis strategy integrating CoT distillation, trajectory-format rewriting, and format unification, resulting in the MMathCoT-1M dataset and the URSA-7B model, which demonstrates state-of-the-art performance on multiple multimodal mathematical benchmarks.
- c. Virgo [12]: Explores a straightforward approach to implementing multimodal slow-thinking systems by fine-tuning a capable MLLM with a small amount of textual long-form thought data, demonstrating that such reasoning processes can be effectively transferred to MLLMs.

4. *Large-Scale Multimodal Pre-Training:*

- a. InfiMM-Math [59]: Introduces InfiMM-WebMath-40B, a high-quality dataset comprising 24 million web pages, 85 million associated image URLs, and 40 billion text tokens, aiming to improve MLLMs’ mathematical reasoning through large-scale multimodal pre-training.

5. *Reinforcement Learning with Verifiable Rewards:*

- a. LMM-R1 [20]: Proposes a two-stage rule-based reinforcement learning framework, LMM-R1, which enhances the reasoning capabilities of 3B-parameter Large Multimodal Models (LMMs) by first strengthening foundational reasoning using text-only data, then generalizing these abilities to multimodal domains. It achieves significant performance improvements even with limited data.
- b. MM-Eureka [48]: Develops the multimodal reasoning model MM-Eureka, which successfully extends large-scale rule-based reinforcement learning to multimodal settings. It reproduces key characteristics of DeepSeek-R1, such as steady increases in accuracy reward and response length during training, and demonstrates superior data efficiency across multiple benchmarks.
- c. R1-VL [18]: Introduces Step-wise Group Relative Policy Optimization (StepGRPO), a novel online reinforcement learning framework that enhances MLLMs’ reasoning abilities through dense step-wise rewards. By incorporating Step-wise Reasoning Accuracy Reward (StepRAR) and Step-wise Reasoning Validity Reward (StepRVR), R1-VL achieves superior performance on various benchmarks by encouraging more structured and logically consistent reasoning processes.

Advanced closed-source MLLMs: Leading proprietary models including GPT-4V [49], GPT-4o [2], and Gemini-1.5-Pro [73] demonstrate exceptional capabilities in multimodal understanding and task-solving, setting benchmarks for open-source alternatives.

Multimodal tree-based methods: Recent works incorporate explicit search mechanisms into multimodal reasoning. AR-MCTS [14] enhances reasoning by combining Monte Carlo Tree Search (MCTS) with active retrieval, improving reasoning space diversity and reliability. Mulberry [15] leverages multi-model collaboration through MCTS’s four iterative operations (selection, expansion, simulation, backpropagation) to identify optimal reasoning paths.

D.3 Implementation Details

We utilize the vLLM framework³ with the following parameters: temperature set to 0.8, top p set to 0.9, and max tokens set to 1024. All experiments were conducted on a machine running Ubuntu 22.04, equipped with NVIDIA A100-80GB GPUs. We list all hyperparameters in Table 9.

Table 9: All hyperparameters utilized in this paper.

Hyperparameter	Value	Description
temperature	0.8	vllm inference settings
top-p	0.9	
top-k	40	
repetition penalty	1.0	
max tokens	1024	
maximum tree depth d_{max}	5	MCTS
exploration weight w	2.0	
predefined terminal threshold c	0.90	
balance factor k	0.95	VOC-based optimal path selection in <i>Sec. 2.2 Phase 2</i>

In the thought card construction stage, during multimodal input-based MCTS iteration, we implement an early termination strategy based on self-consistency for enhanced efficiency. Building on the observation that repeated action sampling at the same state often indicates successful task completion, we terminate simulation early when the model’s consistency score exceeds a threshold c (i.e., $SC(s) > c$). Our experiments show that using a parallel strategy on an A100-80G, acquiring reasoning paths for 500 samples takes only approximately 50 minutes, making this computational overhead minimal compared to large-scale training approaches.

Additionally, we use Problem Condition Complexity (PCC) and Text-Image Semantic (TIS) for problem attributes clustering in card construction; **these computational overheads are also manageable**. Specifically, this overhead consists of two components:

- PCC Cost: The overhead comes from using an MLLM to derive prior known conditions. A lightweight Qwen2-VL-2B model is sufficient for this process, keeping costs manageable.
- TIS Cost: The CLIP-ViT-B-16 (149M) model [34] is computationally efficient. Furthermore, semantic embeddings for 500 seed samples can be pre-computed once (averaging less than 1s per sample), which is a fixed computational overhead. As test samples increase, the amortized CLIP encoding cost per sample diminishes, keeping the actual overhead manageable.

In the inference stage, we evaluate AStar’s effectiveness across both LLM and MLLM architectures. For MLLMs, we can directly utilize their native visual understanding and reasoning capabilities for visual parsing. For traditional LLMs like Qwen2.5-7B, we employ Qwen2-72B-VL solely for visual information extraction, deliberately avoiding its visual reasoning capabilities. This design choice ensures that the inference backbone remains the primary reasoning component while maintaining computational efficiency.

E Supplementary Results

This section presents supplementary results and analysis: E.1 Detailed Results on Multimodal Reasoning Benchmarks, E.2 Comparison with Strong Baselines, E.3 Weak-to-strong Generalization, and E.4 Statistical Significance.

E.1 Detailed Results on Multimodal Reasoning Benchmarks

We provide detailed test results based on various mathematical abilities using the MathVista benchmark. As shown in Table 10, AStar demonstrates notable strengths in statistics and challenging logic,

³<https://github.com/vllm-project/vllm>

whereas other models exhibit superior performance in algebraic and geometric problem-solving. Notably, with Qwen2-VL-2B as our inference backbone, our 2B model even surpasses larger models such as InternLM-XComposer2-VL-7B and Math-LLaVA, achieving performance comparable to GPT-4V. This indicates that, regardless of model size, our AStar reasoning framework effectively enhances multimodal reasoning capabilities.

Table 10: Results on MathVista *testmini* detailed mathematics capabilities. The best results of closed-source MLLMs are highlighted in green. The best and second-best results of open-source MLLMs are highlighted in red and blue respectively.

Model	#Params	ALL	ALG	ARI	GEO	LOG	NUM	SCI	STA
<i>Baselines</i>									
Random Choice	-	17.9	25.8	13.8	22.7	13.4	8.8	15.8	14.3
Human Performance	-	60.3	50.9	59.2	51.4	40.7	53.8	64.9	63.9
<i>Closed-source MLLMs</i>									
Qwen-VL-Plus [74]	-	43.3	39.1	32.0	39.3	18.9	26.4	59.0	56.1
GPT-4V [49]	-	49.9	53.0	49.0	51.0	21.6	20.1	63.1	55.8
<i>Open-source General MLLMs</i>									
LLaVA-1.5-13B [53]	13B	25.7	19.6	28.6	17.6	10.8	27.8	33.6	22.9
InternLM-XComposer2-VL-7B [54]	7B	47.8	32.0	51.6	30.5	13.5	43.8	37.7	62.8
SPHINX-MoE [52]	8× 7B	42.3	31.7	41.6	30.5	16.2	27.1	50.8	50.8
DeepSeek-VL [55]	7B	34.9	29.2	38.8	27.2	18.9	43.1	35.3	33.2
InternVL2-8B [46]	8B	58.3	59.8	56.4	60.3	10.8	30.6	59.0	68.8
Qwen2-VL [45]	7B	58.9	44.1	57.5	43.1	24.3	41.7	66.4	75.1
<i>Open-source Math MLLMs (Large-Scale Training)</i>									
G-LLaVA [56]	7B	25.1	36.0	19.4	37.6	15.2	17.7	21.0	15.1
Math-LLaVA [47]	13B	46.6	51.5	40.7	56.2	23.3	34.7	47.7	42.3
Multimath-7B [60]	7B	50.0	61.9	42.2	64.9	23.3	32.6	42.6	49.2
Math-PUMA-Qwen2-7B [57]	7B	47.9	47.7	46.2	47.3	21.6	32.6	42.6	55.8
URSA-7B	7B	59.8	74.0	53.5	77.4	21.6	35.4	58.2	57.1
AStar (Ours, Training-free Reasoning)	7B	64.2	69.0	63.8	71.7	59.5	60.0	48.2	69.1
	2B	49.6	51.0	49.9	53.1	34.7	46.8	41.3	54.3

E.2 Comparison with Strong Baselines

Table 11 provides a performance comparison of our method against leading open-source and closed-source models. AStar with a 7B inference backbone achieves competitive performance with larger MLLMs. Notably, on the challenging MathVision dataset, our approach exhibits substantial improvements. This suggests that while simpler visual tasks may not significantly benefit from structured reasoning strategies—with performance primarily determined by model capacity—our method shows increasing performance advantages on more complex datasets like MathVerse and MathVision, surpassing both InternVL2.5-26B and InternVL2-Llama3-76B models despite their larger parameter counts of 26B and 72B respectively.

We also benchmark our approach against recent powerful multimodal reasoning methods, including LLaVA-CoT [10] and Virgo [12]. As shown in Table 12, comparative experiments across different model scales demonstrate that our AStar reasoning framework, which effectively integrates MLLMs’ inherent reasoning capabilities with external reasoning guidelines, achieves superior performance with minimal prior data. On challenging datasets like MathVerse, our method exhibits substantial improvements, with the 2B model achieving comparable performance to the extensively trained Virgo 7B model. Further analysis reveals two key insights: First, methods relying on vast solution spaces often struggle to identify appropriate reasoning paths, analogous to finding a needle in a haystack. Second, approaches dependent on large-scale training data typically face difficulties in fully capturing complex long-chain reasoning patterns through implicit learning. In contrast, our method adaptively identifies suitable reasoning strategies based on problem complexity, enabling efficient inference across diverse scenarios.

However, when integrated with the AStar framework, both models demonstrate robust performance across difficulty levels, with Qwen2-VL-7B showing particularly promising results. The larger model

maintains consistent performance even on level-5 problems (the most challenging), achieving an accuracy of 24.8% compared to 26.5% on level-1 problems. This relatively small performance gap between the easiest and hardest problems suggests that AStar effectively bridges the model’s internal implicit reasoning capabilities with external explicit reasoning strategies, enabling more reliable problem-solving across varying complexity levels.

Table 11: Comparison with leading LLMs. The best results are highlighted in **bold**. Results for off-the-shelf models are sourced from corresponding official websites.

Model	MathVista	MathVerse	MathVision	Average
<i>Closed-Source Models</i>				
GPT-4o-0513 [2]	63.8	50.2	30.4	48.1
GPT-4V [49]	49.9	54.4	24.8	43.1
Gemini-1.5-Pro [73]	63.9	35.3	19.2	39.5
Claude-3.5-Sonnet [75]	67.7	-	-	-
<i>Open-Source Models</i>				
Qwen2-VL-72B [45]	70.5	41.3	25.9	45.9
InternVL2.5-26B [46]	67.7	40.1	28.0	45.3
InternVL2-Llama3-76B [46]	65.5	42.8	23.7	44.0
Astar (Qwen2.5-7B)	64.2	53.9	32.7	50.3
Astar (Qwen2-VL-7B)	61.7	47.5	26.8	45.3

Table 12: Comparison with recent works targeting enhanced multimodal reasoning through structured thinking. We list 2B and ≥ 7 B-scale baselines. The best results in each box are highlighted in **bold**. Our method demonstrates significant performance improvements.

Model	Size	MMStar	ChartQA	MathVista	MathVerse
<i>2B-Scale Baselines</i>					
Mulberry [15]	2B	51.3	77.7	51.7	-
Astar (Qwen2-VL-2B)	2B	52.0	78.6	49.6	35.6
<i>≥ 7B-Scale Baselines</i>					
Insight-V [11]	7B	61.5	81.5	59.9	-
AR-MCTS [14]	7B	-	-	64.1	-
Mulberry [15]	7B	61.3	83.9	63.1	-
LLaVA-CoT [2]	11B	57.6	-	54.8	-
LlamaV-o1 [27]	11B	59.6	-	54.4	-
URSA [13]	7B	55.4	-	59.8	45.7
Virgo [13]	7B	-	-	-	37.5
Astar (Qwen2.5-7B)	7B	62.3	84.2	64.2	53.9
Astar (Qwen2-VL-7B)	7B	61.7	83.9	61.7	47.5

E.3 Weak-to-Strong Generalization

As described in prior works [76], interactions between weak and strong models can be categorized into three primary paradigms: 1) weak-to-strong improvement, where models with limited capabilities can effectively guide the development of more advanced models, 2) self-improvement, wherein the weak and strong models are identical, focusing on designing methods to enhance the model’s

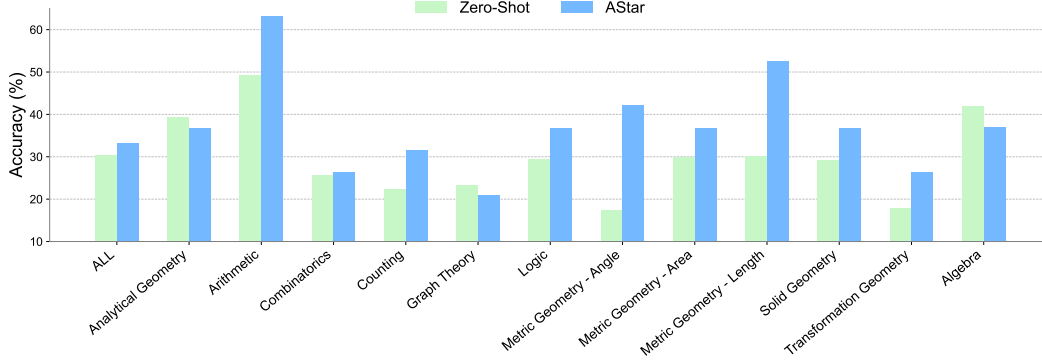


Figure 11: Weak-to-strong generalization results: Performance comparison of GPT-4o in zero-shot and AStar-enhanced (Qwen2-VL-7B guidance) settings across various dimensions of MathVision. The results demonstrate that a weaker model (Qwen2-VL-7B) can effectively guide a stronger model (GPT-4o) through the AStar framework, validating the framework’s potential for weak-to-strong generalization in mathematical reasoning tasks.

own performance, and 3) knowledge distillation, which involves transferring the capabilities or knowledge from strong models to weak models. Through our main results, where thought cards are constructed based on Qwen2-VL-7B, we have already demonstrated the significant potential of our AStar method in knowledge distillation (Qwen2-VL-7B \rightarrow Qwen2-VL-2B) and self-improvement (Qwen2-VL-7B \rightarrow Qwen2-VL-7B).

Therefore, in this section, we empirically evaluate AStar’s effectiveness in weak-to-strong generalization. We hypothesize that a weaker model, when integrated with AStar, can effectively guide a more powerful policy model. To test this hypothesis, we leverage the reasoning guidance (thought cards) generated by Qwen2-VL-7B to assist GPT-4o in solving challenging problems from the MathVision dataset.

As illustrated in Figure 11, we present a comprehensive comparison between GPT-4o’s zero-shot performance and its performance when enhanced with AStar (using Qwen2-VL-7B’s reasoning guidance) across multiple dimensions of the MathVision benchmark. Our results demonstrate that incorporating our reasoning paradigm enables models with limited capabilities to provide valuable supervision to stronger policy models. Notably, the Qwen2-VL-7B model, despite its relatively limited capabilities, successfully guides the more powerful, closed-source GPT-4o. This finding validates the potential of learning from prior reasoning patterns and offers promising insights for developing more scalable and sophisticated strategies to enhance AI reasoning capabilities.

E.4 Statistical Validation

To statistically evaluate the differences between reasoning with and without our AStar paradigm, we apply the nonparametric Wilcoxon signed-rank test [77]. This statistical test is specifically designed to compare two related samples or repeated measurements when the data may not follow a normal distribution, making it particularly suitable for our analysis. The Wilcoxon signed-rank test evaluates whether there is a significant difference between paired observations through the following procedure:

1. **Calculate differences:** For each pair of values X_i and Y_i , compute the difference $D_i = X_i - Y_i$.
2. **Rank differences:** Take the absolute values $|D_i|$ and rank them from smallest to largest, denoted as R_i . For ties, average ranks are assigned.
3. **Assign signs to ranks:** For each pair (X_i, Y_i) , assign the sign of D_i to its corresponding rank: $R'_i = \text{sign}(D_i) \cdot R_i$, where $\text{sign}(D_i) = +1$ if $D_i > 0$, -1 if $D_i < 0$, and 0 if $D_i = 0$.
4. **Calculate rank sums:** Separate the ranks into positive and negative sums: $W^+ = \sum_{D_i > 0} R'_i$ and $W^- = \sum_{D_i < 0} R'_i$.
5. **Determine test statistic:** The test statistic W is the smaller of the two sums: $W = \min(W^+, W^-)$.

6. **Calculate p-value:** The p-value is derived from the distribution of the test statistic W .

In our analysis, we test the null hypothesis of no significant difference (H_0 : difference = 0) against the alternative hypothesis of a significant difference (H_1 : difference \neq 0). We compare model performance across multiple dimensions, including overall accuracy, per-category accuracy (MathVista, MathVerse, and MMMU), and accuracy at different difficulty levels (MathVision). For example, in MathVista, we contrast accuracy scores obtained by Qwen2-VL-2B in two conditions: (1) baseline reasoning (e.g., accuracy for all dataset, algebra, logical reasoning, etc.), and (2) AStar-powered reasoning across the same dimensions.

Following common practice, we use a significance level of 0.05 (5e-2). As shown in Table 13, all p-values are below 0.05, leading us to reject the null hypothesis (H_0). These findings offer strong statistical evidence that incorporating our AStar paradigm significantly enhances reasoning performance across all tested dimensions.

Table 13: Statistical significance of differences between reasoning with and without AStar reasoning paradigm.

Model	MathVista	MathVerse	MathVision	MMMU
Qwen2-VL-2B	2.7e-4	1.5e-2	4.9e-4	6.1e-4
Qwen2-VL-7B	3.4e-3	2.6e-2	5.5e-4	2.5e-4

F Case Study

Taking a geometry problem in MathVerse as an example, we provide a qualitative comparison of LLaVA-NeXT-8B [53], Qwen2-VL-7B [45], and AStar-7B in Figure 12. The results demonstrate that LLaVA-NeXT-8B and Qwen2-VL-7B struggle to accurately parse complex geometric relationships, leading to potential errors in each step of their reasoning processes. In contrast, our AStar framework effectively combines MLLMs’ internal implicit reasoning capabilities with external explicit reasoning guidelines. This integration exhibits explicit and well-defined reasoning steps with comprehensive understanding, ultimately arriving at the correct solution.

G Further Discussions

Discussion on Why Our Method Outperforms GPT-4o. Our experimental results demonstrate that AStar outperforms GPT-4o on challenging multimodal reasoning benchmarks despite utilizing a significantly smaller backbone model. This counterintuitive advantage stems from several key factors: (1) AStar’s thought cards effectively decompose complex reasoning processes into manageable components, allowing our model to focus on executing individual reasoning steps rather than handling entire problem trajectories simultaneously; (2) While GPT-4o relies predominantly on implicitly encoded reasoning patterns, AStar’s external high-level reasoning guidelines create a complementary cognitive scaffold that orchestrates the problem-solving process; and (3) Our retrieval mechanism dynamically selects appropriate thought cards based on problem attributes, enabling task-specific adaptation without resource-intensive training. These findings suggest that strategic integration of explicit reasoning guidance with implicit model capabilities represents a promising direction for advancing multimodal reasoning beyond simply scaling model parameters or training data.

Broader Impact. Multimodal reasoning plays a crucial role in real-world applications. This paper proposes an efficient MCTS-based automated reasoning paradigm that achieves strong performance while significantly reducing computational and energy costs. This research advances our understanding of MLLM reasoning capabilities, paving the way for more responsible and scalable AI development.

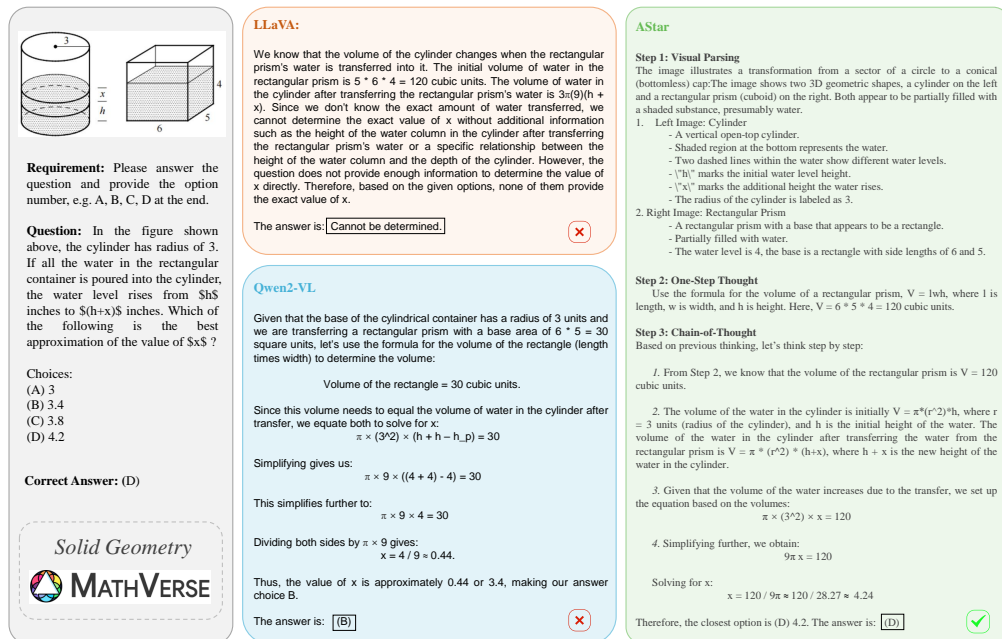


Figure 12: Qualitative comparison of reasoning processes across different models. AStar demonstrates superior understanding through its explicit, well-structured reasoning steps, leading to accurate solution derivation. The comparison highlights AStar's ability to systematically decompose complex geometric relationships while maintaining reasoning clarity throughout the problem-solving process.